NACA TN 4163

NATIONAL ADVISORY COMMITTEE FOR AERONAUTICS

TECHNICAL NOTE 4163

EFFECT OF TEMPERATURE ON ROLLING-CONTACT FATIGUE LIFE WITH LIQUID AND DRY POWDER LUBRICANTS

By Thomas L. Carter

Lewis Flight Propulsion Laboratory
Cleveland, Ohio

NACA

Washington
January 1958

NATIONAL ADVISORY COMMITTEE FOR AERONAUTICS

TECHNICAL NOTE 4163

EFFECT OF TEMPERATURE ON ROLLING-CONTACT FATIGUE LIFE WITH LIQUID AND DRY POWDER LUBRICANTS

By Thomas L. Carter

SUMMARY

The effect of temperature using di(2-ethylhexyl)sebacate lubricant and dry powder lubricants on rolling-contact fatigue life of AISI M-1 tool-steel balls was investigated in the rolling-contact fatigue spin rig at maximum theoretical Hertz stress levels of 650,000 and 725,000 pounds per square inch in compression. In tests at temperatures of 100° F, 250° F, and 450° F using the sebacate lubricant it was found that life decreased with increasing temperature. Metallurgical transformation tended to increase in intensity with the total number of stress cycles and with test temperature.

Tests were also made at 450° F using dry molybdenum disulfide and dry graphite powders as lubricants. The molybdenum disulfide was carried into the test zone as a suspension in polyalkylene gylcol which evaporated at 350° F. Ball life at 450° F with both molybdenum disulfide and graphite powders was significantly reduced from that observed with a fluid lubricant under the same test conditions. Failure was by fatigue spalling, but it had a different appearance than spalling previously observed with fluid lubricants. The failures appeared to be caused by stress raisers localized in the bands of pure rolling. The stress raisers probably were the dry lubricant particles. Since a complete bearing has better conformity between ball and race curvatures, hence greater relative sliding of the surfaces, the observed effect of dry lubricant particles acting as stress raisers may be reduced to a negligible role in normal rolling-contact bearing applications.

At 100° F the glycol suspension of molybdenum disulfide produced results for short lived balls in the same range as plain glycol and other fluid lubricants. An abrupt increase in slope of the fatigue life curve was observed at 2×10^8 stress cycles. This change in slope appeared to be due to a combination of higher than normal surface shear stresses and corrosion cracking.

INTRODUCTION

One of the primary considerations in developing bearings able to sustain the high temperatures encountered in present and anticipated aircraft gas-turbine engines is the fatigue life of the bearing elements. Aside from loads carried and design considerations, the fatigue life is affected by the materials used in the bearing elements and the substance used to provide lubrication. At moderate temperatures (to 350° F) proven steels and lubricants are available for satisfactory performance. However, at temperatures demanded by designers of present and anticipated engines (ref. 1), these standard materials lose their hot hardness and dimensional stability, and the lubricants break down into less desirable substances.

Substances are available that will provide lubrication at higher temperatures. In the tool steels there is a wide selection of available alloys that do not lose hardness or dimensional stability at temperatures anticipated by the bearing industry. However, research is necessary to choose the optimum lubricants and materials from the standpoint of adequate rolling-contact fatigue life. The large bulk of information accumulated in the NACA rolling-contact fatigue program and by research workers elsewhere has been carried out at moderately elevated or room temperatures. The main evaluation of lubricants at high temperatures has pertained to their effects on friction and wear. The published information on fatigue life of materials in rolling contact under dry powder lubrication is especially limited. Since this class of lubricants has the widest useful temperature range, it is felt that information in this category would be very desirable.

This report presents the effect of temperature with a fluid lubricant and the effect of dry powder lubricants at high temperature on the rolling-contact fatigue life of AISI M-1 tool-steel balls. M-1 tool steel was chosen for this program because it is one of the more promising tool steels and because it is also the one on which the most information has been secured at room temperature.

APPARATUS

Only brief descriptions of the apparatus and procedure are given here. A more detailed presentation can be found in reference 2 and the appendix. Figure 1(a) is a cutaway view of the rolling-contact fatigue spin rig. The two test balls were propelled by air jets and revolved in a horizontal plane on the bore surface of a hardened tool-steel cylinder (fig. 1(b)).

The loading on the balls was produced by centrifugal force, and the stress was calculated according to the methods of reference 3.

Approximately 15 milliliters per hour of lubricant were introduced in droplet form into the drive airstream between the guide plates. The fast moving airstream had an atomizer effect, and the lubricant was reduced to a fine mist that adhered to surfaces to provide a lubricating film. Graphite flow was controlled by a dust-generating chamber described in the appendix. Flow rates were low, of the order of 0.1 ounce per hour.

Orbital speed was measured by counting the pulses from a photoamplifier with an electronic tachometer. A ball or race failure resulted in the generation of an increased signal from a velocity pickup attached to the rig. This signal, when amplified, actuated a meter relay that shut down the system.

Temperature was controlled by mixing heated air with the normal drive air supply. The test temperature and temperature control signal were taken from thermocouples on the top and bottom of the race cylinder.

All ball test specimens were from the same heat of AISI M-1 air-melt tool steel and had a nominal 1/2-inch diameter. The running track was predetermined by grinding two diametrically opposed 3/16-inch flats on the ball surface. Race cylinders were AISI M-1 vacuum-melt tool steel.

PROCEDURE

Before the test all race cylinders were given dimensional, surface-finish, and hardness inspections. All test balls were weighed and given a surface examination at a magnification of 36. A record was kept of any abnormalities in surface conditions at the running track. Prior to inspection and use, test specimens were flushed and scrubbed with 100 percent ethyl alcohol and clean cheesecloth. During storage they were protected by a corrosion-resistant-oil film. Care was taken during assembly not to scratch the running surfaces. The bore surface and test balls were coated with lubricant during assembly.

The rig was brought up to operating speed as rapidly and as smoothly as possible. About 30 minutes were required for the hot airstream to heat the test cylinder to the test temperature when running at 450° F. Speed, air pressure, temperature, and vibration levels were recorded during the test. Total running time was recorded and converted into total stress cycles on the ball specimen. A post-test surface examination at a magnification of 36 was made to observe track conditions.

Failure data were plotted on Weibull paper, which is a distribution of the log log of the reciprocal of the portion unfailed against the log of the stress cycles to failure. This distribution function developed by Weibull fits the observed scatter in the fatigue lives of rolling-contact bearings (ref. 4). Because of the usually small sample (about

30 balls) involved, the data cannot reliably be fitted into a frequency curve. Instead, the cumulative form of the distribution is used. The cumulative distribution function (Weibull) is as follows:

$$\log \frac{1}{S(L)} = GL^e \qquad (1)$$

where $S(L)$ is the fraction of the sample surviving the first L stress cycles, and G and e are positive constants.

Figures presenting ball life results use special probability paper on which the Weibull distribution becomes a straight line of slope e. The ordinate represents log-log $1/S(L)$ but is graduated in terms of the fraction failed at L stress cycles.

A set of data is ordered according to life, and each succeeding life is given a rank (statistical percentage) and is plotted on Weibull paper. If the median rank is used, a line is drawn that takes the general direction of the array of points and splits the array in half. A median rank is an estimate of the true rank in the population that has an equal probability of being too large or too small.

A table of median rank values for sample sizes up to 20 and formulas for calculation of the median rank values for any order position in any sample size are given in reference 4.

As with any measurement, the confidence in this data is limited by its statistical reliability. With rolling-contact fatigue data the wide scatter normally encountered necessitates large sample sizes in order to establish accurately the relation of life against percent survival shown in the Weibull plot. At the same time, expense and duration of each test limit the practical number of specimens that can be evaluated. Confidence limits for the data produced in this program were calculated by the method of Lieblein (ref. 5).

RESULTS AND DISCUSSION

Effect of Temperature with the Sebacate Lubricant

The data produced in this portion of the investigation are a representation of the effect of increased temperature upon the rolling-contact fatigue life of air-melt AISI M-1 tool-steel balls when lubricated with a synthetic sebacate. Table I tabulates the properties of the liquid lubricant. The AISI M-1 air-melt ball material was obtained from Latrobe heat number 13-801 and contained 0.8 percent carbon, 4 percent chromium, 1 percent vanadium, 1.5 percent tungsten, and 8 percent molybdenum. Test temperatures were 100°, 250°, and 450° F. Ball loading was held

at a level that produced a maximum theoretical Hertz compressive stress of 650,000 pounds per square inch and a maximum shear stress of 195,000 pounds per square inch 0.008 inch below the surface.

The 100° F run was made to establish a base line for comparison with higher temperature results. The results are shown in figure 2. Track surface appearance and subsurface metallographic appearance were very similar to that observed with other lubricants for M-1 and other materials at 100° F (ref. 6). The failures produced were of the same type as those commonly observed in full-scale bearings. A comparison of a spin rig fatigue spall with one typical of full-scale bearings is made in figure 3. They are both characterized by being localized in nature, limited in depth of spalling and of subsurface origin near the plane of maximum shear stress. The fatigue life results observed at 100° F are similar to fatigue data previously secured with a sebacate lubricant.

The life results produced at 250° and 450° F are shown in figures 4(a) and (b), respectively. The life results for M-1 and the sebacate lubricant at the test temperatures of 100°, 250°, and 450° F are summarized in figure 4(c).

An examination of the fatigue failures produced at 250° and 450° F did not reveal any contrast in appearance or origin with those produced at 100° F. An examination of the running track surface did not reveal any significant evidence of chemical corrosion. At all three temperatures the tracks exhibited the tendency to darken with increased running time; this is characteristic of spin rig specimens. Only a slight tendency of this darkening to increase with higher test temperature was observed.

The formation of a transformation product in the subsurface zone of maximum shear stress in AISI M-1 tool-steel spin rig specimens was reported in reference 6 at room and 200° F test temperatures. Since these observations were for the same heat of material as used in this report, no further investigation was made for the 100° and 250° F specimens. Metallographic sections were made with the 450° F test specimens, and typical results are presented in figure 5. Only slight troostitic transformation was observed at room temperature. At 200° F this transformation became more pronounced. At 450° F a further increase in this transformation was observed, although it was not as significant as would have been expected from the contrast between room temperature and 200° F. This troostitic transformation increases with test temperature and with the number of stress cycles applied to the specimen.

Figure 4(c) shows a reduction in early failure lives with increased test temperature. One cause of the lower life would be the lowering of the lubricant viscosity with increased test temperature. The reduction in fatigue life with a reduction in lubricant viscosity was reported in

reference 7. Table II shows the theoretical reduction in ball life due to viscosity reduction using the relation of reference 7. The observed lives in figure 4(c) were less than those expected if viscosity of the lubricant were the only variable affecting fatigue life. The difference between the observed and the theoretical lives is probably caused by other factors that are amplified at higher test temperatures. One possible example would be the deterioration of the metallographic structure due to troostitic transformation. A reduction in life with increased test temperature for the longer lived balls greater than that anticipated from viscosity effects was observed for the 250° F test. However, this reduction did not continue at the 450° F test temperature.

At 450° F the sebacate used in this series tended to polymerize into a very viscous residue. The rate of formation was low, but in the longer test runs there was an appreciable accumulation of this substance on the ball track. Figure 6 is a photograph of this condition. Since viscosity affects fatigue life, the formation of a very viscous film with longer test time would tend to extend fatigue life, and this effect would be more pronounced for longer lived fatigue failures. This lubricant breakdown limited the test temperature feasible with the sebacate.

A trend toward shorter rolling-contact fatigue life greater than that anticipated from temperature lowering of viscosity alone was observed. However, an analysis of this effect must be tempered by confidence in the statistical reliability of the data. For the sample sizes of 21, 16, and 8 balls each, used to produce the data in figures 2, 4(a), and 4(b), these confidence limits are wide in relation to the observed difference in lives. However, if no effect exists on life with increasing temperature, the probability for the 10-percent lives of the three plots falling in ascending order is only 1 in 6. This is so because each of the lines was calculated by the least-squares, best-fit technique so that they are objective. Thus, the observed lowering of fatigue life with increasing temperature has an 83-percent probability not to have been caused by chance.

Dry Powder Lubricants

Dry powders were used in an attempt to find lubricants usable at test temperatures beyond 450° F. In preliminary test runs when powders were introduced as a dust in air, problems in metering during prolonged unattended periods were encountered so that in subsequent tests a suspension of the powder in a fluid that would evaporate at the test temperature was used. A polyalkylene glycol that evaporates at about 350° F and leaves little residue was chosen for the tests run at 450° F. The same heat of AISI M-1 tool steel was used for test specimens as in the previous series with the sebacate. The properties of the polyalkylene glycol used in this test series are given in table I. The dry powders

used had a maximum particle size of 25 microns. Runs at 100° F were made with a plain glycol and a 0.2-percent suspension of molybdenum disulfide powder in glycol to establish a basis for comparison with high-temperature results. The molybdenum disulfide suspension was then run at 450° F where the glycol evaporated, leaving only the dry powder present. In these test runs ball loading was held at a stress level that produced a maximum theoretical Hertz stress of 725,000 pounds per square inch and a maximum shear stress of 225,000 pounds per square inch 0.009 inch below the surface. A run of dry graphite at 450° F was made at a stress level of 650,000 pounds per square inch compression and 195,000 pounds per square inch shear 0.008 inch below the surface.

Polyalkylene glycol at 100° F. - The results for the plain polyalkylene glycol at 100° F are shown in figure 7(a); this run was made to establish a base line for comparison with results for a solid-particle suspension in the fluid. Subsurface metallographic appearance was very similar to that observed with other lubricants for M-1 and other materials at 100° F (ref. 6 and previous section). However, the track surface did not have the characteristic darkening due to an adherent oxide film that was characteristic of all previous material-lubricant combinations tested in the spin rig. This could have been due to abrasion or inhibited oxide formation. Since the track did not show signs of appreciable wear, the latter cause appears more logical. Failure appearance and type were the same as other spin rig failures and those common to full-scale bearings. The life results were similar to those produced with the sebacate at 100° F (fig. 2, adjusted for stress: Life = $K(1/\text{stress}^{10})$), ref. 8).

0.2-Percent molybdenum disulfide suspension in polyalkylene glycol at 100° F. - The results shown in figure 7(b) were produced at 100° F for comparison with the pure fluid and with high-temperature results. A best-fit straight line has been drawn through the data points, but, obviously, two straight lines (dashed lines) are required to fit the data points reasonably well. The shorter lived specimens apparently produce a curve that is of about the same life and slope as the glycol and other fluid lubricants. However, at about 2×10^8 stress cycles there appears to be an increase in slope of the fatigue life curve. This condition produced by a unique type of lubricant (i.e., solid-particle suspension) indicated that the cause of failure may be different in this case from previously observed fatigue failures with fluid lubricants.

An extensive metallographic investigation was conducted in an attempt to explain the changes in slope of the fatigue life curve observed at 2×10^8 stress cycles. Figure 8 shows running track appearance and longitudinal cross sections of the subtrack region for three specimens subjected to successively greater numbers of stress cycles. Figures 8(e) and (f) show a failed specimen with the complete fatigue spall. This spall is limited in depth and appears to originate in subsurface shear

as do normal fatigue spalls observed in the spin rig and in full-scale bearings. However, the depth of origin of the spalls is confined to a zone less than 0.002 inch below the ball surface. A zone of 0.004 to 0.009 inch is considered normal for the failures observed in previous specimens run with simple fluid lubricants (ref. 6). A large amount of cracking was observed at a depth of much less than 0.001 inch (fig. 8(g)). Incipient cracking and matrix damage originating from carbides were more common and more agglomerated than in previous specimens. This indicated both higher local stresses and nonuniform stressing. Structural changes characteristic of the subsurface zone of maximum shear tended to be less severe and closer to the surface.

A strong tendency for formation of surface cracking was observed in these specimens (figs. 8(b), (d), and (f)). This condition is not typical of fluid lubricant fatigue failures. This cracking had a characteristic pattern that bore a definite relation to the relative sliding always encountered in rolling contact of a ball with a race. Since the radius of rotation is at a maximum at the running track center and is progressively less toward the outside while the angular rotation is the same, the surface speed must vary in the transverse direction. This causes relative sliding of the surfaces. To maintain an over-all rolling of the ball, the sum of the friction forces generated at the contact zone must be zero. Otherwise the ball would skid. Thus, the sliding is opposite the rolling direction at the center of the ball and in the same direction at the track edges. At some point in between, the relative sliding of the two surfaces is zero. Thus, there are two bands of pure rolling on the track. The cracking in figures 8(b), (d), and (f) has an abrupt change in direction at these bands of pure rolling. Thus, it has a characteristic pattern relative to surface sliding.

The shallow depth of subsurface crack origin (figs. 8(a), (c), (e)) and the surface crack pattern (figs. 8(b), (d), and (f)) indicate a much stronger skin effect in the suspension lubricated balls than that observed in fluid lubricated balls. High shear stresses are apparently generated at the surface by the relative sliding of the contact surfaces. This is in addition to the high shear stress that results from the compressive stresses and that is a maximum about 0.009 inch below the surface. Since the relative sliding and contact pressures are the same for this test run as for previous fluid lubricated runs, the effective friction coefficient apparently is higher for the solid-particle-suspension lubricant.

Evidence of corrosion at the contact surface was very strong in this test run. All previous fluid lubricated runs yielded very limited evidence of contact surface corrosion. Figures 8(b), (d), and (f) show this pitting and the tendency for it to aline with the surface cracking. Apparently there is an interaction between surface corrosion and the cracking, with each one promoting the other. Cracking, or the high

local stresses causing cracking, would facilitate corrosion, and a corrosion pit would provide the stress concentration for fatigue cracking. Figures 8(a) and (c) present a cross section of the ball subsurface showing the penetration of corrosion cracking into the subsurface. The increase in depth with longer test time is apparent. These corrosion cracks generate secondary cracking parallel to the surface, which is the normal cause of fatigue spalling. A typical spall is shown in figure 8(e).

The formation of very small fatigue spalls is shown in figure 8(d). These fine spalls are too small to cause enough vibration for failure shutdown, but they are of interest because of their unique tendency to form at the bands of pure rolling. This observation, together with the indication that higher than normal localized stresses were present, as indicated by agglomerated incipient failures (fig. 8(d)), indicated that some stress-raising effect was acting in the bands of pure rolling. This could be the solid lubricant particles in the suspension. This observation will be developed further in the discussion of the next test run.

The abrupt change in slope of the fatigue curve observed in figure 7(b) for the molybdenum disulfide - polyalkylene glycol suspension appears to be caused by an interaction of stress corrosion and the high surface shear stresses due to skin effects. The higher shear stress generated by surface sliding would tend to move the maximum shear stress nearer the surface than would be normal for that resolved from compressive stresses alone. The corrosion cracking progresses from the surface at a relatively constant rate. When it reaches the critical zone (i.e., high shear stress) where fatigue spall cracking originates, the susceptibility for fatigue failure is greatly increased and a large fatigue spall will soon develop. The time for corrosion cracking to proceed to this depth corresponds to the running time for 2×10^8 to 4×10^8 stress cycles (regions of increased slope in fig. 7(b)) and hence the concentration of the last eight failures within this range.

Dry molybdenum disulfide powder at 450° F. - The results shown in figure 9(a) were produced at a test temperature of 450° F with molybdenum disulfide suspended in polyalkylene glycol. The glycol evaporated at 350° F and left a dry powder at the test temperature.

A best-fit straight line was drawn through the data points of figure 9(a), but again, as for the molybdenum disulfide suspension results at 100° F, it is obvious that two straight lines (shown as dashed lines) are required to fit the data points reasonably well. In these tests reaching the test temperature required about 30 minutes. Since heat is supplied by the drive air, preheating was not practical. A running time of 30 minutes corresponds approximately to the intersection of the two dashed lines so that the lower dashed line corresponds to a transition from room temperature to 450° F. Once the test temperature was reached,

the slope changed and produced the results considered to be a measure of AISI M-1 tool steel lubricated with dry molybdenum disulfide powder at 450° F.

The life observed at these test conditions was poorer than that observed at the same test temperature with the sebacate fluid (fig. 4(b)) after adjusting the life to correct for stress differences. The disparity in life is even greater when comparing with room-temperature results. Apparently some new and adverse factor, which did not exist with a fluid lubricant, is influencing fatigue life.

At the elevated temperature it is possible that corrosion is greatly accelerated. Sulfur compounds could be formed because of the decomposition of molybdenum disulfide to form corrosive substances. Chemical activity observed for the molybdenum disulfide suspension at 100° F would be accelerated by temperature, and this corrosion damage would appear to be a logical cause.

Dry graphite powder at 450° F. - In order to evaluate possible chemical corrosion action as a failure-causing factor, a comparison can be made with test results produced with dry graphite powder. Since graphite is quite different from molybdenum disulfide chemically but similar physically, different results would be expected if chemical activity were a major factor in ball fatigue life. The results shown in figure 9(b) were produced at 450° F with dry graphite powder. These tests were run at a lower stress level (650,000 psi) than the molybdenum disulfide runs previously discussed; however, an adjustment can be made to the stress level of the molybdenum disulfide run (725,000 psi) by the relation $\text{Life} = K(1/\text{stress})^{10}$ established for the spin rig in reference 8. The number of data points is limited because of the problems encountered in metering the graphite-air dust, but the close proximity of the points to a straight line indicates that the results may closely approximate the results for a greater number of points. Since no fluid was present at the test temperature and the particle size was the same (25 microns) for both powders, the molybdenum disulfide and graphite powder lubricants closely resembled each other physically.

Comparison of Results with Fluid and Dry Powder Lubricants

Figure 10 is a comparison of the Weibull plots for the two dry powders with each other and with fluid lubricants all at the same stress level. AISI M-1 tool steel showed the poorest fatigue at 450° F. The similarity of results for the two dry powder lubricants that have greatly different chemical characteristics appears to minimize the importance of chemical corrosion as a factor causing rolling-contact fatigue failure at these test conditions. One possible reason for this apparent anomaly is the lack of a fluid film to hold corrosive substances at the contact surfaces. Volatile sulfur oxides would be removed by the air blast if

not held in solution. In addition, all but two of the failures in the tests at 450° F with the glycol - molybdenum disulfide suspension occurred before 2×10^8 stress cycles where stress corrosion became an important factor in the 100° F tests. Figure 11(a) shows no evidence of corrosion pitting as compared with that noted at 100° F (figs. 8(b) and (d)). While the two test runs with dry powder lubricants at 450° F produced similar results, they are much different from the results for the fluid sebacate at 450° F and the fluids and suspensions at 100° F.

The metallographic transformation in the subsurface zone of maximum shear for both molybdenum disulfide and graphite lubricated balls is similar to that characteristic of rolling-contact fatigue specimens in general. The light etching area of figure 11(b) is similar to that observed with a sebacate fluid at 450° F (fig. 5). Metallographic changes do not appear to be the cause of the lower life.

The most logical explanation of the low rolling-contact fatigue life produced with the dry powders appears to be in mechanical rather than chemical effects. Both the dry powders produced failures that were mutually identical in appearance yet entirely different from those observed with the fluid lubricants. Figure 11 illustrates this point. A pattern of two annular bands of fine spalling was observed on the ball track. These bands were coincident with the bands of pure rolling that are present in all spheres rolling on a cylindrical surface. These spalls in the bands of pure rolling are similar to the normal fatigue spall except that they are on a much smaller scale. They appear to originate from subsurface shear cracking as do normal spalls. A tendency for small spalls to form in the bands of pure rolling was noted previously with the molybdenum disulfide suspension at 100° F (fig. 8(d)). A metallographic examination showed that the incipient failures and matrix damage originating from carbides tended to be more common and more segregated than in previous examinations (ref. 6), which indicates that high localized stresses were present. Figure 11(b) shows localized matrix damage. These localized areas tended to be under the bands of pure rolling. This indicates that a stress raiser was acting in the bands of pure rolling. If an even pressure distribution were present, the maximum pressure would be at the center of the track and the first sign of failure would be expected there.

Apparently the lack of relative sliding of the contacting surfaces at the bands of pure rolling enables the dry lubricant particles to retain some of their shape while the sliding in the remainder of the contact area smears the particles into a smooth continuous lubricating film. This phenomenon is illustrated schematically in figure 12. The pressure distribution with a fluid lubricant is smooth and reaches a maximum at the center of the contact ellipse. This is the typical pressure distribution for a sphere in contact with a cylinder as computed from reference 3.

The existence of a dry particle which is larger than the average thickness of the lubricating film formed by the smearing action would produce the effect shown in figure 12(b). Since at the bands of pure rolling the relative motion of the two surfaces is perpendicular to the plane of the surfaces, all stresses on the lubricant particles would be in compression. The particles would have to be deformed to the average film thickness by compressive forces. The particles could bear stresses higher than their normal yield strength for the same reason that the balls carry stresses far above their normal yield strength through what is essentially hydrostatic loading; that is, the material has no place to which to flow. A mathematical analysis of this phenomenon would be very complex, if not impossible.

The theory that the dry lubricant particles produce high, localized compressive stresses in the bands of pure rolling is a hypothetical one, but there is a substantial amount of evidence indicating that some type of localized stress raiser is present that was not present in fluid lubricants. The unique appearance of the spalling, intense localized incipient matrix damage confined to the region of the unique spalling, and the low life all indicate that this is the case. Since a complete bearing has better conformity between ball and race, hence greater relative sliding of the surfaces, the observed effect of dry powder lubricant particles acting as stress raisers may be reduced to a negligible role in normal rolling-contact bearing applications.

SUMMARY OF RESULTS

A group of air-melt AISI M-1 tool-steel balls was tested under rolling-contact conditions in the fatigue spin rig. The effect of increased liquid lubricant temperature was observed when run with di(2-ethylhexyl)sebacate at a maximum theoretical Hertz stress of 650,000 pounds per square inch maximum in compression and 195,000 pounds per square inch maximum in shear 0.008 inch below the surface. The results of this investigation are as follows:

1. A trend toward lower rolling-contact fatigue life with increasing temperature was observed in the range studied (100° to 450° F).

2. Metallurgical transformation in the subsurface zone of maximum shear tended to increase with test temperature and the number of stress cycles.

The same group of AISI M-1 balls was tested with a polyalkylene glycol at 100° F and a molybdenum disulfide - polyalkylene glycol suspension at 100° and 450° F at a maximum theoretical Hertz compressive stress of 725,000 pounds per square inch and a maximum shear stress of 225,000 pounds per square inch 0.009 inch from the ball surface. A

check run was made with graphite powder at 450° F and the same stress level as the runs lubricated with the synthetic sebacate. The results of this investigation are as follows:

1. With dry powder lubricants at 450° F the failures appeared to be hastened by stress raisers localized in the bands of pure rolling. The stress raisers probably were the dry lubricant particles. The fatigue life was reduced from that observed with a fluid lubricant under the same test conditions. Corrosion at the track surface and metallographic transformations did not appear to play a significant role in the observed lowering of life. Failure was by fatigue spalling, but it had a different appearance than spalling previously observed with fluid lubricants. Since a complete bearing has better conformity between ball and race, hence greater relative sliding of the surfaces, the observed effect of dry powder lubricant particles acting as stress raisers may be reduced to a negligible role in normal rolling-contact bearing applications.

2. Molybdenum disulfide - polyalkylene glycol suspension at 100° F produced results for short lived balls in the same range as plain glycol and other fluid lubricants. An abrupt increase in slope of the fatigue life curve was observed at 2×10^8 stress cycles. This change in slope appeared to be due to a combination of higher than normal surface shear stress and corrosion cracking. The corrosion cracking progressed from the track surface at an approximately constant rate in all balls. When it reached the critical subsurface shear zone, failure quickly resulted. The minimum time for this penetration corresponded to approximately 2×10^8 stress cycles.

Lewis Flight Propulsion Laboratory
National Advisory Committee for Aeronautics
Cleveland, Ohio, October 16, 1957

APPENDIX - APPARATUS AND PROCEDURE

Test Rig

As was previously stated, figure 1(a) is a cutaway view of the rolling-contact fatigue spin rig. The test specimens are the two balls revolving in a horizontal plane on the bore surface of a hardened tool-steel cylinder (fig. 1(b)). Air at pressures to 100 pounds per square inch is introduced through the nozzles to drive the balls at high orbital speeds. The nozzle system and the cylinder are held in place by upper and lower cover plates fastened by three removable bolts. The rig assembly is supported from a rigid frame by three flexible cables. In order to keep external constraint at a low value, the drive air is introduced into the rig through a 6-foot-long flexible metal hose.

Operation. - The two test balls separate and maintain relative positions 180° apart at speeds above the critical frequency. A detailed analysis of the rig operation may be found in reference 2.

Loading. - The only loading on the balls is that produced by centrifugal force. No contact is made with the ball test specimen except by the race cylinder at the contact ellipse. The load can exceed 700 pounds for a 1/2-inch steel ball revolving in a 3.25-inch bore race cylinder at an orbital speed of 30,000 rpm. At this speed a maximum Hertz stress of approximately 750,000 pounds per square inch compression will be developed at the center of the contact ellipse.

Lubrication. - In this investigation three lubrication systems were used. The standard system developed originally for the rig was used for fluids, while new systems were developed to meet the requirements of solid-particle - liquid suspension and dry solid-particle lubricants.

The introduction of fluid lubricant was accomplished by introducing droplets of the lubricant into the drive airstream between the guide plates (fig. 1(a)). The rotating airstream atomizes the droplets and carries the lubricant to all surfaces. Lubricant flow rate is controlled by regulating the pressure upstream of a long capillary tube. The pressure drop through the capillary was sufficient to give excellent control of the flow for small flow rates. The lubricant flow rate used in this series of tests was approximately 15 milliliters per hour.

For the introduction of solid particles in fluid suspensions, the system shown in figure 13 was employed. A simple regulation of flow by a valve in the line is not feasible because of the tendency for suspended particles to clog the valve after a prolonged period of running. In the system shown in figure 13 a pressure drop exists between the lubricant reservoir and the test area because of the static-pressure drop caused by the velocity of the airstream surrounding the test balls. This pressure

drop is about 4 millimeters of mercury ($P_A - P_1$). This provides the driving force for lubricant flow from the reservoir to the test area. By providing an orifice in the line and controlling the rate of air bleeding into the line upstream of the orifice, the pressure drop across the capillary tube ($P_A - P_2$) can be controlled. Thus, the rate of lubricant flow is controlled by a valve through which it does not pass. The flow of bleed air carries the suspension rapidly into the test chamber and prevents evaporation of the suspension vehicle before it gets into the test chamber. This system was found to be a very reliable method of metering solid-particle suspensions over prolonged periods of time (72 hr) without attention.

Dry solid lubricant particles were suspended in an airstream with a turbulent air dust generator. This air suspension was drawn into the test rig by the pressure drop caused by the high-velocity air driving the balls. Considerable difficulty was experienced in maintaining a consistent flow rate during extended periods without attention. This is a disadvantage with a test rig designed to operate overnight unattended.

Instrumentation. - Three major instrumentation systems provide for speed measurement and control, temperature measurement and control, and failure detection and shutdown.

Orbital speed of the balls is measured by counting the pulses from a photoamplifier on an electric tachometer. The pulses are generated by the two test balls interrupting a light beam focused on the photocell. A voltage proportional to the frequency of the photocell output is fed into a Swartwout Controller that automatically regulates the drive air pressure to maintain the desired orbital ball speed. Temperature is measured with an iron-constantan thermocouple that is in contact with the top of the race cylinder (fig. 1(a)). This is the closest practical location of the thermocouple with relation to the ball running track. A calibration with a thermocouple in the airstream surrounding the balls showed a variation of less than 2 percent with the test temperature. It can be assumed that the race, balls, and surrounding air are all maintained within a narrow temperature range. A second thermocouple contacting the cylinder top provides the signal for the automatic temperature controller. This controller blends room-temperature air with air heated by a 25-kilowatt heater in the proportion necessary to maintain the desired test temperature.

Failures are detected by comparing the amplified signal from a velocity vibration pickup (attached to the rig, see fig. 1(a)) against a predetermined signal level preset over a meter relay. The large vibration amplitude resulting from a ball or cylinder fatigue spall trips the meter relay and results in shutdown of the test and all instrumentation.

Air supply. - The drive air is dried to less than 30-percent relative humidity and then is filtered before being used in the rigs. Pressure of 125 pounds per square inch is maintained by a central centrifugal compression system.

Test Specimens

Cylinders. - The dimensions of the test cylinders are as follows: outside diameter, 4.750 inches; length, 3.00 inches; initial nominal inside diameter, 3.250 inches. The bore surface finish was 2 to 3 microinches for all cylinders. Roundness of the bore was held to 0.0001 inch, and bore taper was held to a maximum of 0.0003 inch. Hardness measurements were taken on the cylinder ends. Each cylinder was uniform within two hardness numbers, although average hardness varied from Rockwell C-60 to C-64 for different cylinders.

Between 10 and 15 tests may be run on a bore surface. The bore is then reground 0.060 inch larger and refinished. This new surface is about 0.022 inch below the location of the maximum shear stress of the previous tests, and the effects of prior stressing are considered to be negligible. Failure positions on one cylinder surface do not correlate with failure positions of the previous test surface.

Test balls. - By taking advantage of the fact that a rotating body free to adjust itself will rotate about the axis of maximum rotational inertia, test balls may be modified so that they will rotate about any fixed axis. All test balls in this series of tests were air-melt AISI M-1 tool steel hardened to Rockwell C-63 to C-64. The axis of rotation of each ball was preselected by grinding two diametrically opposed 3/16-inch flats. This facilitated preinspection of the running track and restarting of the unfailed balls. The axes were selected in a random manner in order to reduce the effect of fiber flow orientation previously reported in reference 9.

Test lubricants. - The sebacate lubricant (di(2-ethylhexyl)sebacate) was taken from a large batch meeting the Air Force MIL-L-7808 specification. This lubricant, which has been used in bulk lubrication of full-scale bearings at outer-race temperatures exceeding 600° F (ref. 10), broke down under the severe conditions of fine dispersion existing in this rig when running at 450° F. The graphite powder had a particle size of 25 microns.

The molybdenum disulfide suspension was a commercial preparation which was a 1-percent by weight suspension of molybdenum disulfide in a water-base glycol. This was then diluted with four parts of polyalkylene glycol to make a suspension of 0.2-percent molybdenum disulfide by weight. This concentration provided the desirable amount of dry lubricant to

maintain a continuous film on the running track and provided a high enough flow rate of the glycol vehicle to introduce the lubricant into the test chamber.

Pretest Inspection

Cylinders were given dimensional, surface-finish, and hardness inspections. This was followed by a magnetic particle inspection for both cracks and large subsurface inclusions and a visual inspection for deep scratches and other mechanical damage.

All test balls were weighed and given an inspection at a magnification of 36. Excessive scratches or pitting and any cracks, laminations, or flat spots were noted in a permanent record.

Prior to inspection and use, test specimens were flushed and scrubbed with 100 percent ethyl alcohol and clean cheesecloth. This procedure left a thin film of grease on the surface, but this was considered desirable to minimize corrosion.

Assembly of Rig

The rig and test specimens were cleaned and assembled with care to prevent scratching of the bore surface. The bore surface and test balls were coated with lubricant.

Starting and Running Procedure

The rig was brought up to operating speed as rapidly and as smoothly as possible. The rig could then be switched to automatic speed control or left on manual control. On manual control the rig speed must be corrected at intervals to compensate for the speed increase due to run-in of the test specimens. Run-in is rapid for the first few minutes and is practically complete after the first 2 hours. Rig temperature reached equilibrium at the 450° F test temperature in about 20 minutes. The control system automatically maintained the desired temperature.

Speed, temperature, and oil flow were monitored regularly. Speed, temperature, air pressure, and vibration levels were recorded at each reading. The test was continued until a predetermined number of stress cycles had been exceeded or until a ball or race failure actuated the meter relay which shut down the rig.

Stress Calculations

With ball weight, speed, and orbital radius of rotation of the test balls known, the load can be calculated. The stress developed in the contact area was calculated from the load and specimen geometry by using the modified Hertz formulas given in reference 3.

Post-Test Inspection

After failure or a predetermined number of stress cycles, the ball running tracks were examined at a magnification of 36 with a microscope. Any abnormalities that correlated with the fatigue life results were noted and followed up with a further metallographic investigation. Specimens were mounted in Bakelite, ground to the desired cross section, polished, and etched to reveal subsurface metallographic structure. Some inspections of the running track surfaces after a polish with diamond dust were made to determine corrosion pitting and its relation to crack formation.

REFERENCES

1. SAE Panel on High-Speed Rolling-Contact Bearings: Trends of Rolling-Contact Bearings as Applied to Aircraft Gas-Turbine Engines. NACA TN 3110, 1954.

2. Macks, E. F.: Fatigue Spin Rig - A New Apparatus for Rapidly Evaluating Materials and Lubricants for Rolling Contact. Lubrication Eng., vol. 9, no. 5, Oct. 1953, pp. 254-258.

3. Jones, A. B.: New Departure - Analysis of Stresses and Deflections. Vols. I and II. New Departure Div., General Motors Corp., Bristol (Conn.), 1946.

4. Johnson, Leonard G.: The Median Ranks of Sample Values in Their Population with an Application to Certain Fatigue Studies. Ind. Math., vol. 2, 1951, pp. 1-9.

5. Lieblein, Julius: A New Method of Analyzing Extreme-Value Data. NACA TN 3053, 1954.

6. Bear, H. Robert, and Butler, Robert H.: Preliminary Metallographic Studies of Ball Fatigue Under Rolling-Contact Conditions. NACA TN 3925, 1957.

7. Carter, Thomas L.: Effect of Lubricant Viscosity on Rolling-Contact Fatigue Life. NACA TN 4101, 1957.

8. Butler, Robert H., and Carter, Thomas L.: Stress-Life Relationship of the Rolling-Contact Fatigue Spin Rig. NACA TN 3930, 1957.

9. Butler, Robert H., Bear, H. Robert, and Carter, Thomas L.: Effect of Fiber Orientation on Ball Failures Under Rolling-Contact Conditions. NACA TN 3933, 1957.

10. Anderson, William J.: Performance of 110-Millimeter-Bore M-1 Tool Steel Ball Bearings at High Speeds, Loads, and Temperatures. NACA TN 3892, 1957.

TABLE I. - LIQUID LUBRICANT PROPERTIES

Viscosity, centistokes (a)				Viscosity index		Neutralization number (a)	
Before		After		Before	After	Before	After
100° F	210° F	100° F	210° F				
Di(2-ethylhexyl)sebacate[b]							
		13.50	4.91		232		0.15
Polyalkylene glycol							
8.62	2.27	8.75	2.28	75.8	72.6	1.03	1.05

[a]Samples taken from reservoir at beginning of first test run and after completion of test series.

[b]MIL-L-7808B.

TABLE II. - THEORETICAL LOSS IN LIFE DUE TO TEMPERATURE LOWERING VISCOSITY

Test temperature, °F	Lubricant viscosity, centistokes	10-Percent life (observed)	10-Percent life (theoretical)	Life ratio, $\frac{\text{Observed}}{\text{Theoretical}}$	50-Percent life (observed)	50-Percent life (theoretical) (b)	Life ratio, $\frac{\text{Observed}}{\text{Theoretical}}$
100	13.5	15.7×10^6	[a]15.7×10^6	1	580×10^6	[a]580×10^6	1
250	3.8	10.2×10^6	[b]12.2×10^6	0.84	109×10^6	[b]450×10^6	0.24
450	1.66	4.75×10^6	[b]10.3×10^6	0.46	160×10^6	[b]382×10^6	0.42

[a]Assumed the same as the observed life.

[b]Based upon relation $L_1/L_2 = (\eta_1/\eta_2)^{0.2}$ (ref. 7) where L is life and η is viscosity.

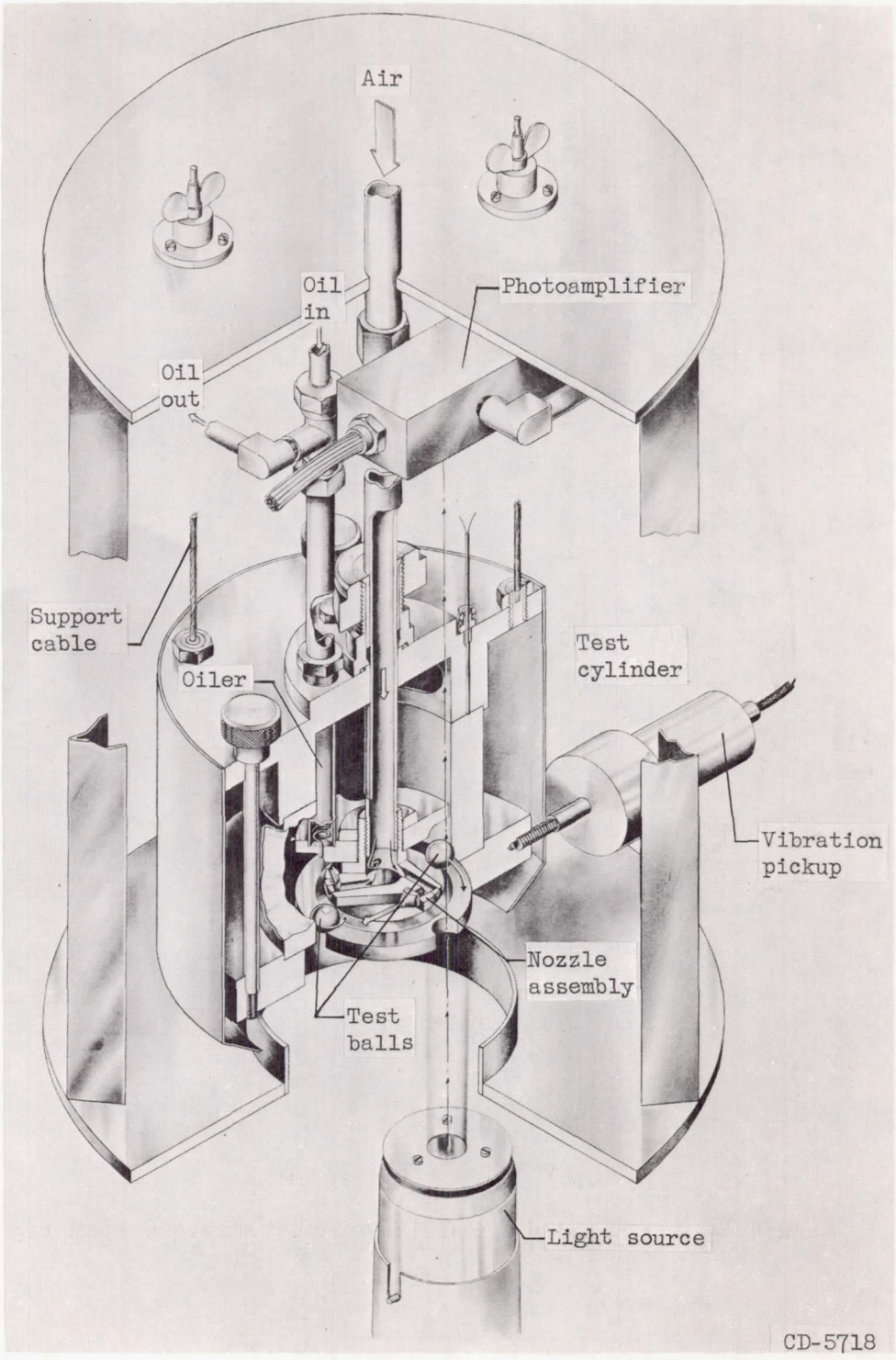

(a) Cutaway view.

Figure 1. - Rolling-contact fatigue spin rig.

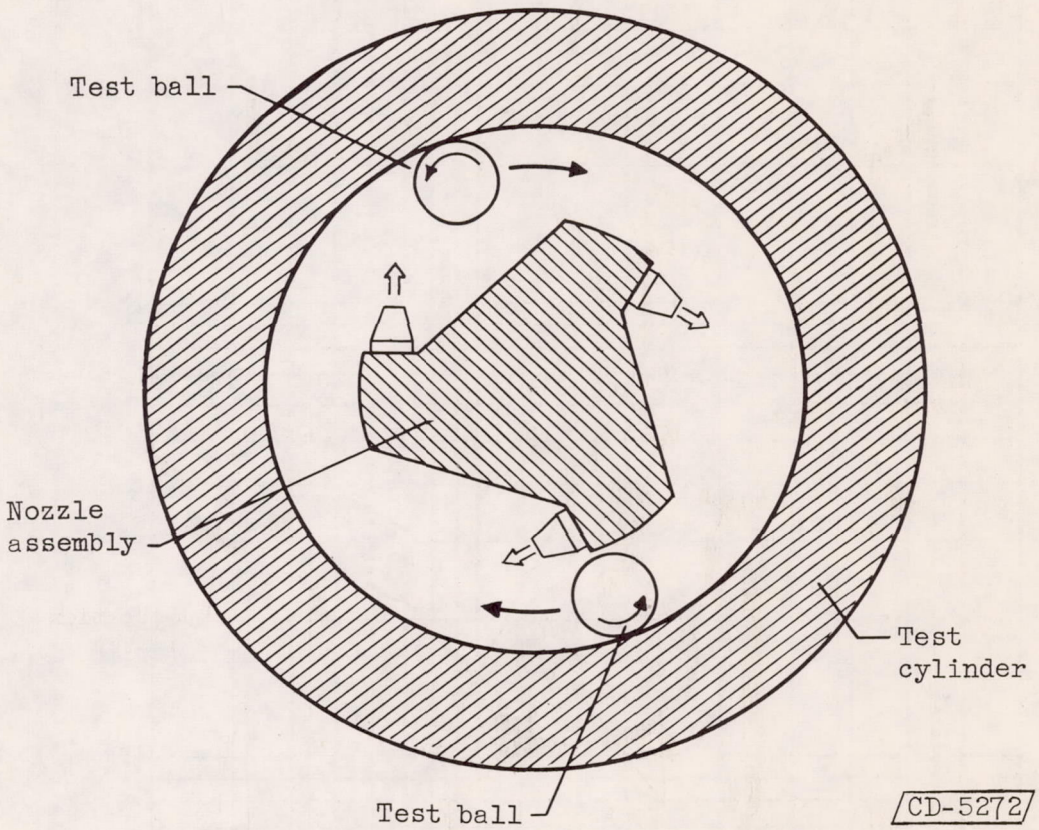

(b) Schematic diagram.

Figure 1. - Concluded. Rolling-contact fatigue spin rig.

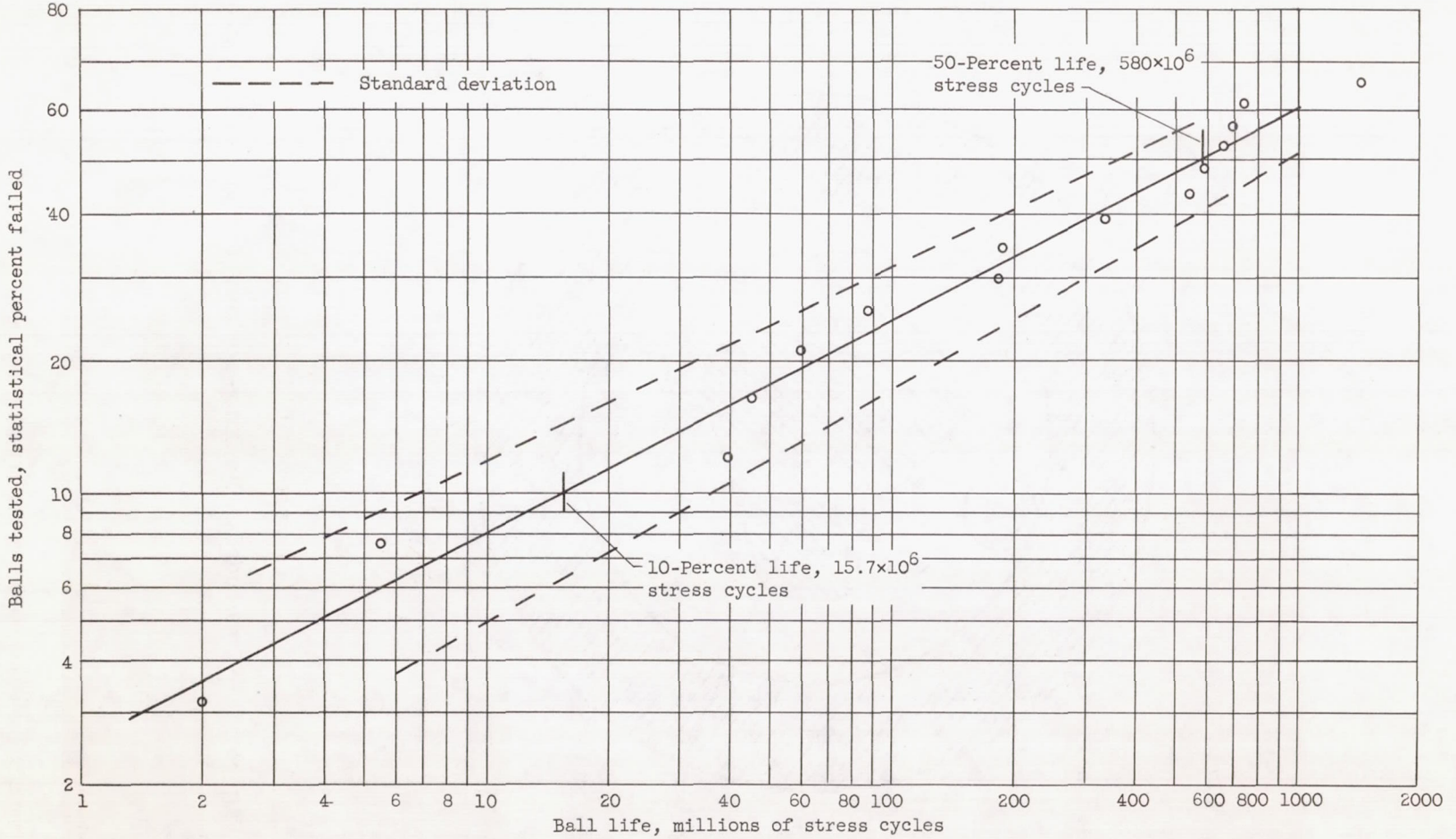

Figure 2. - Fatigue life for 1/2-inch AISI M-1 balls. Lubricant, di(2-ethylhexyl)sebacate; test temperature, 100° F; maximum Hertz compressive stress, 650,000 pounds per square inch.

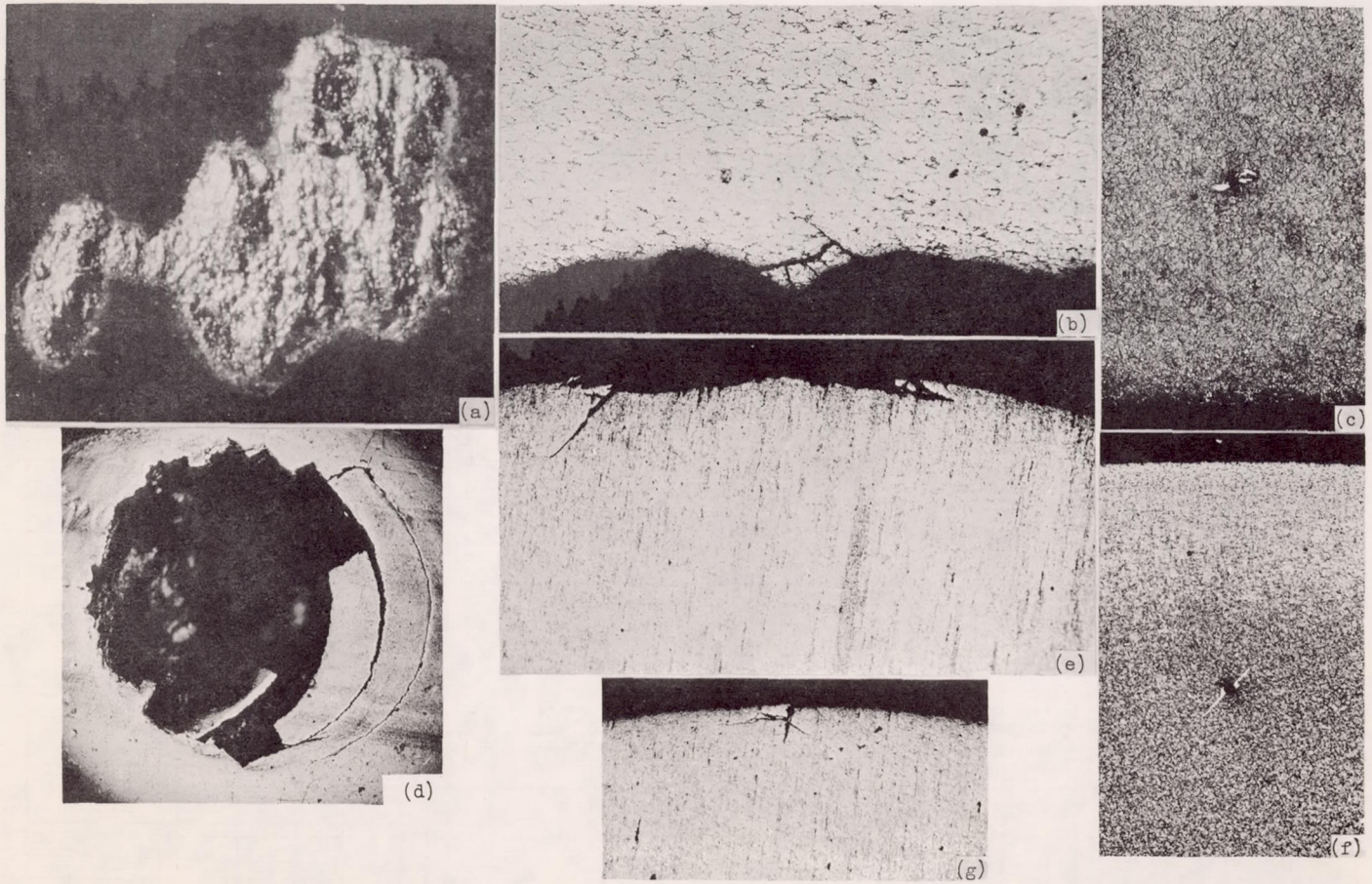

(a) Small spall on inner race of M-1 (222) bearing; X15.
(b) Section view of part of same spall; X37.
(c) Incipient failure near point of maximum shear stress; X100
(d) Typical spall, spin-rig-tested ball; X50.
(e) Section view of spall; X37.
(f) Incipient failure near point of maximum shear stress; X100.
(g) Section view of early failure on spin-rig-tested ball; X50.

Figure 3. - Comparison of failures of a bearing inner race and balls tested in rolling-contact fatigue spin rig.

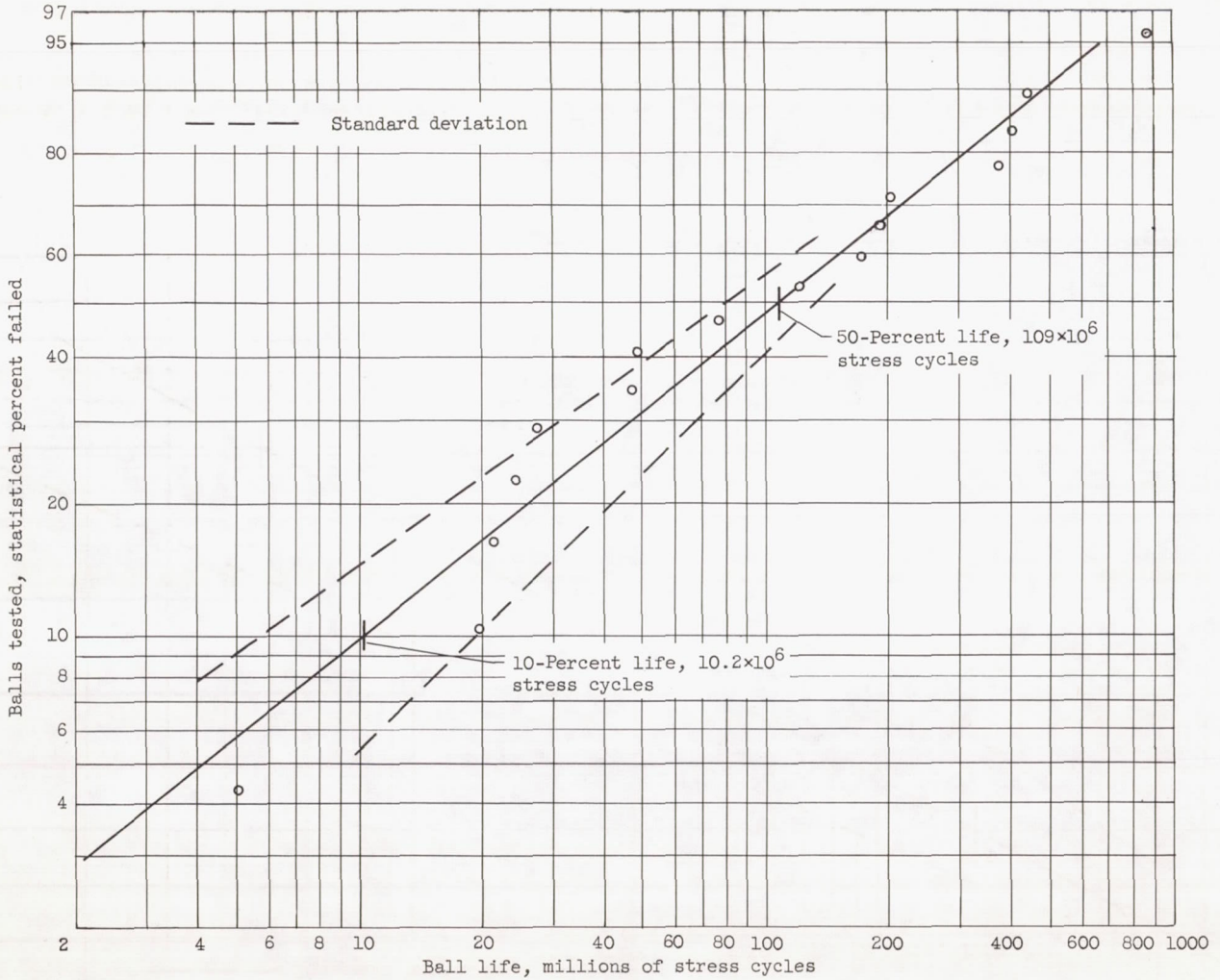

(a) Test temperature, 250° F.

Figure 4. - Fatigue life for 1/2-inch AISI M-1 balls. Lubricant, di(2-ethylhexyl)sebacate; maximum Hertz compressive stress, 650,000 pounds per square inch.

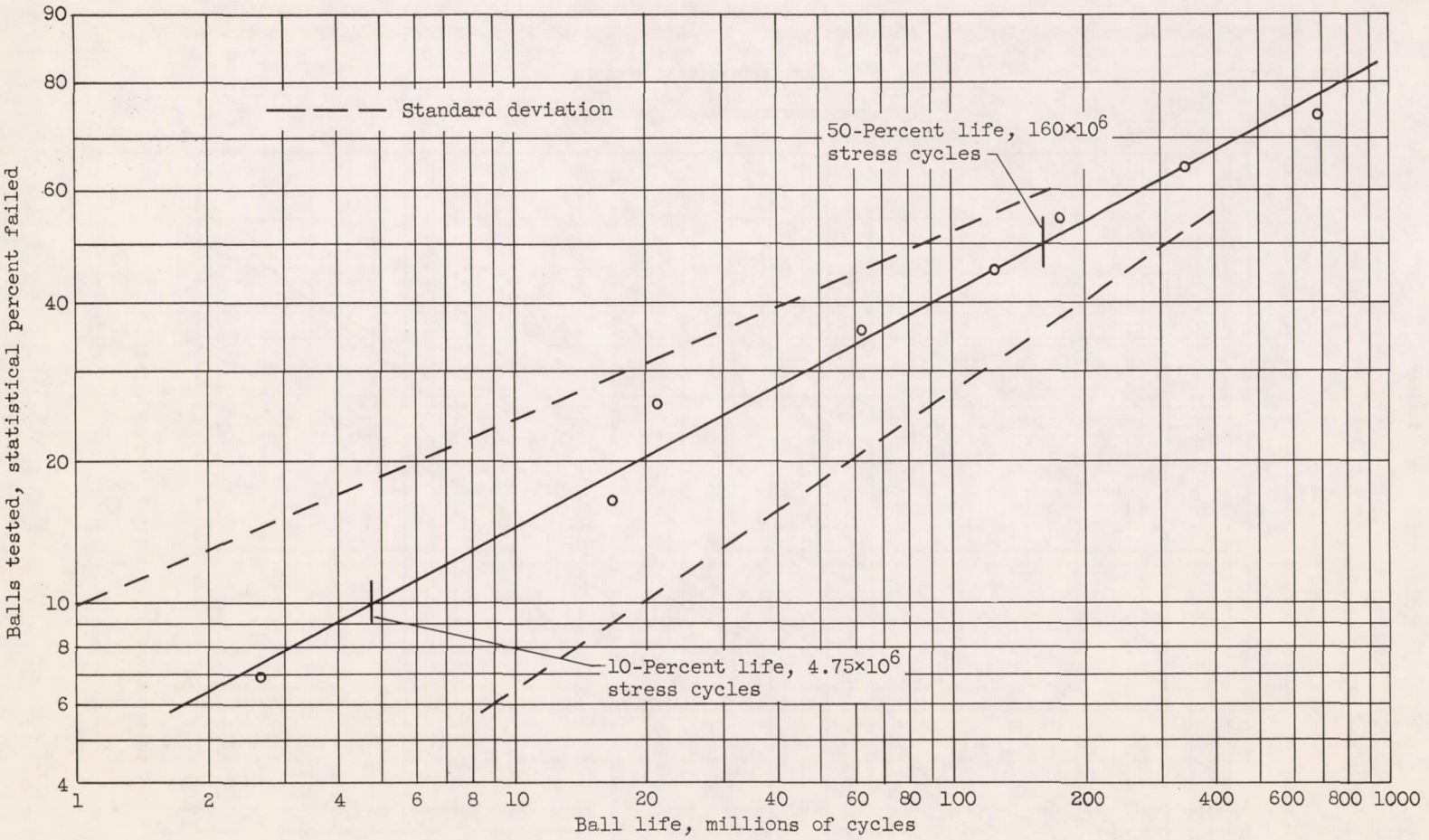

(b) Test temperature, 450° F.

Figure 4. - Continued. Fatigue life for 1/2-inch AISI M-1 balls. Lubricant, di(2-ethylhexyl)sebacate; maximum Hertz compressive stress, 650,000 pounds per square inch.

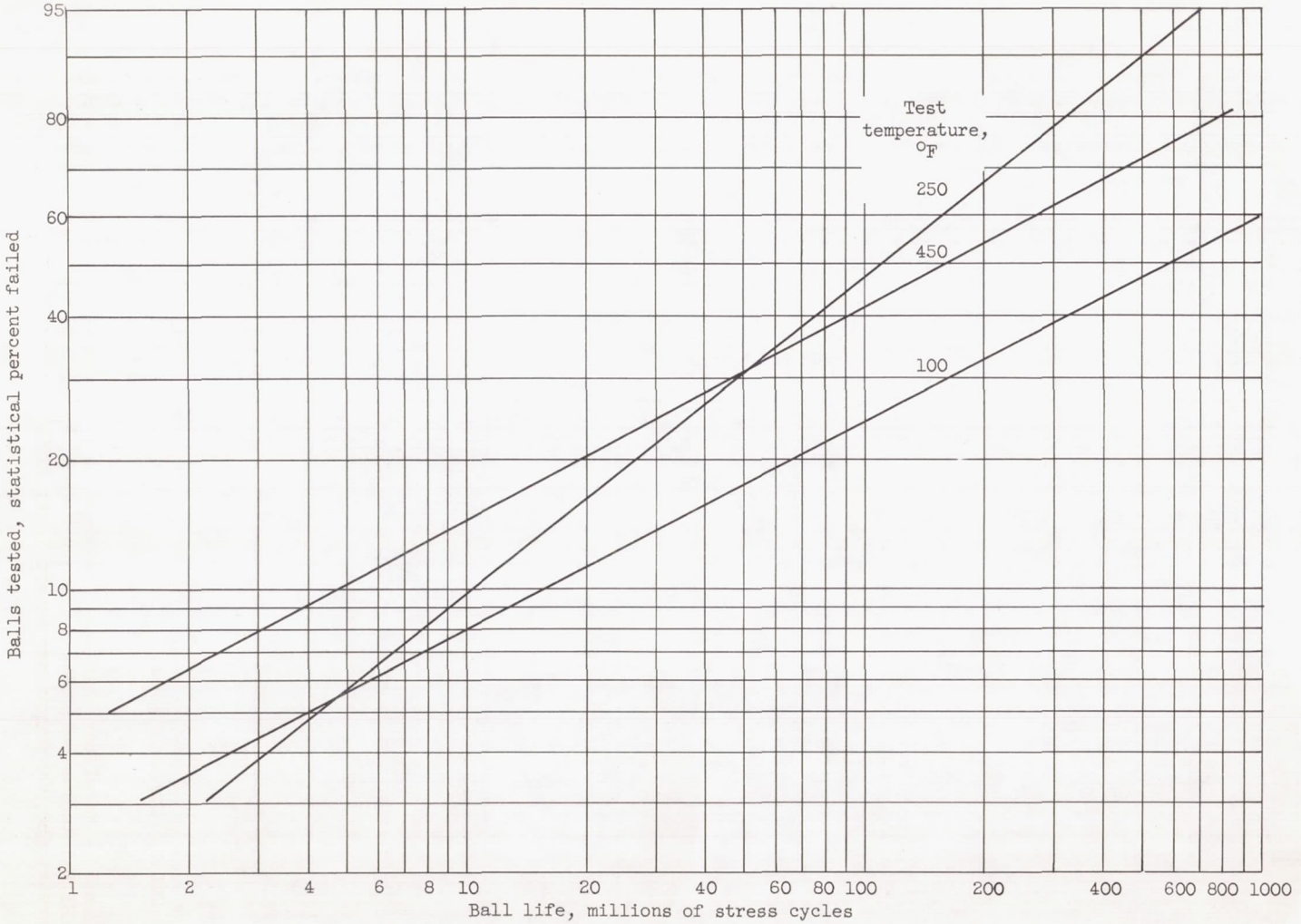

(c) Various test temperatures.

Figure 4. - Concluded. Fatigue life for 1/2-inch AISI M-1 balls. Lubricant, di(2-ethylhexyl)sebacate; maximum Hertz compressive stress, 650,000 pounds per square inch.

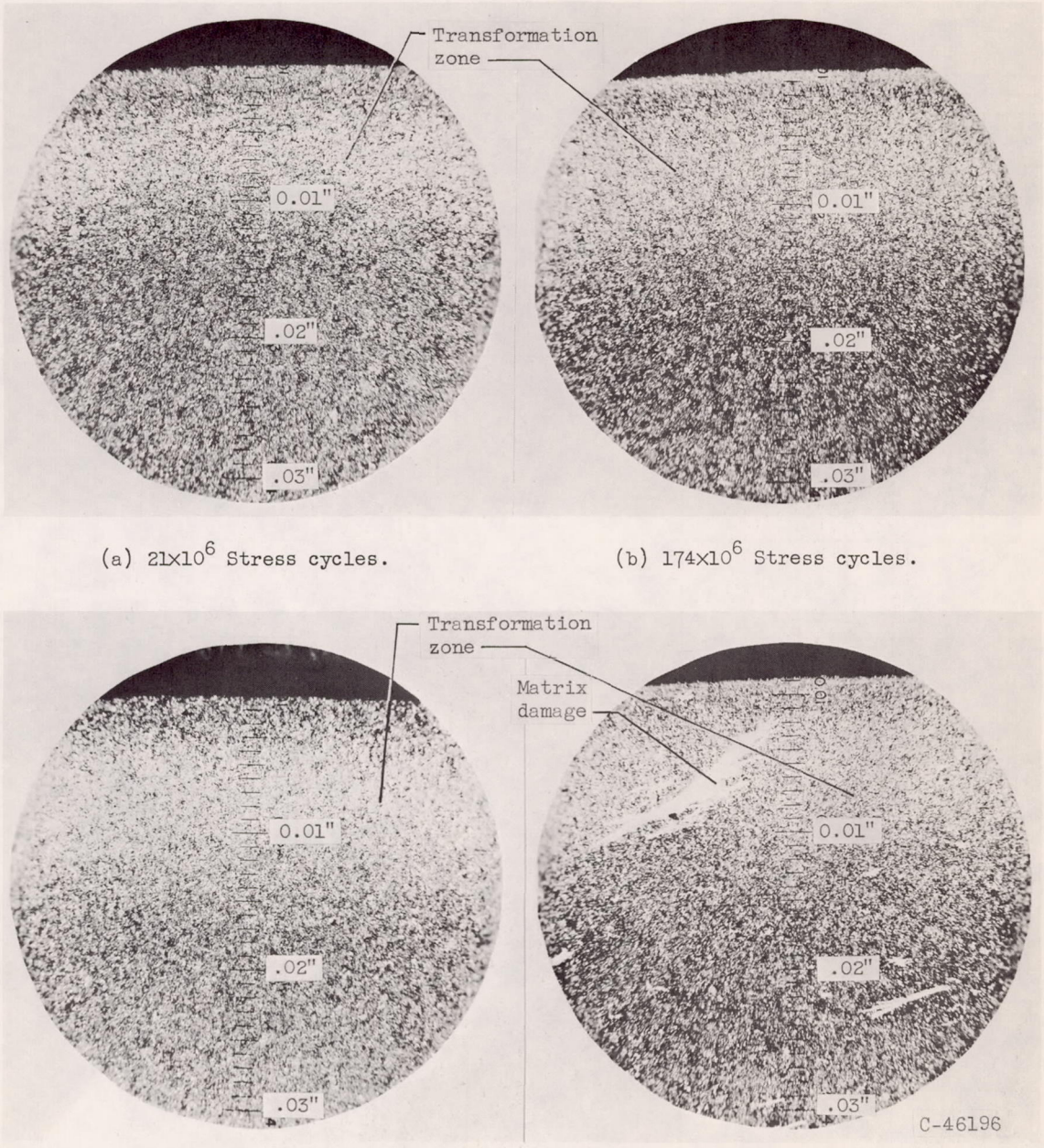

(a) 21×10^6 Stress cycles.

(b) 174×10^6 Stress cycles.

(c) 261×10^6 Stress cycles.

(d) 197×10^6 Stress cycles; matrix damage in shear plane.

Figure 5. - Metallographic transformation in subsurface zone of maximum shear. AISI M-1 tool steel; test temperature, 450° F; maximum Hertz compressive stress, 650,000 pounds per square inch; X100.

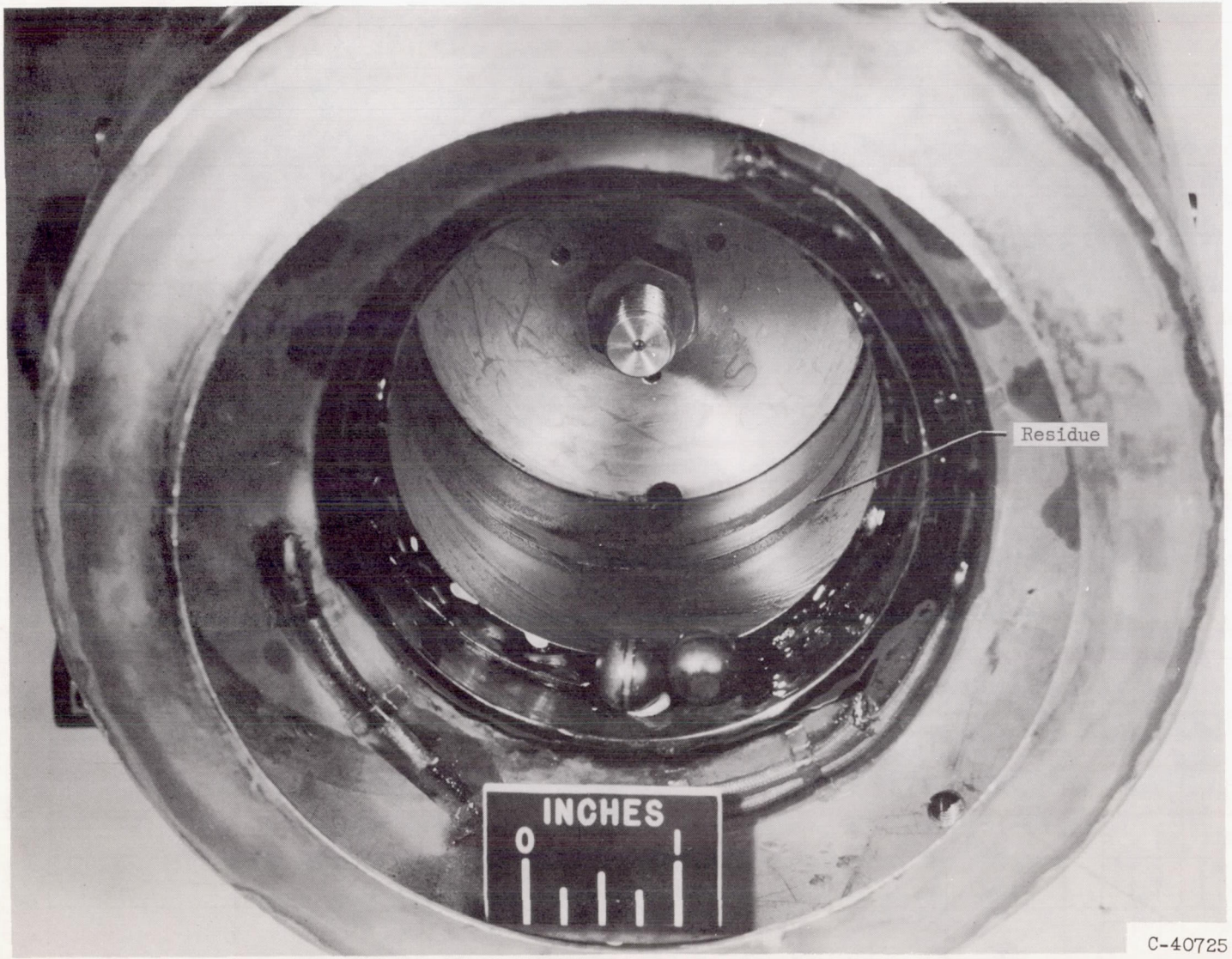

Figure 6. - Viscous residue formed when running with a sebacate at 450° F.

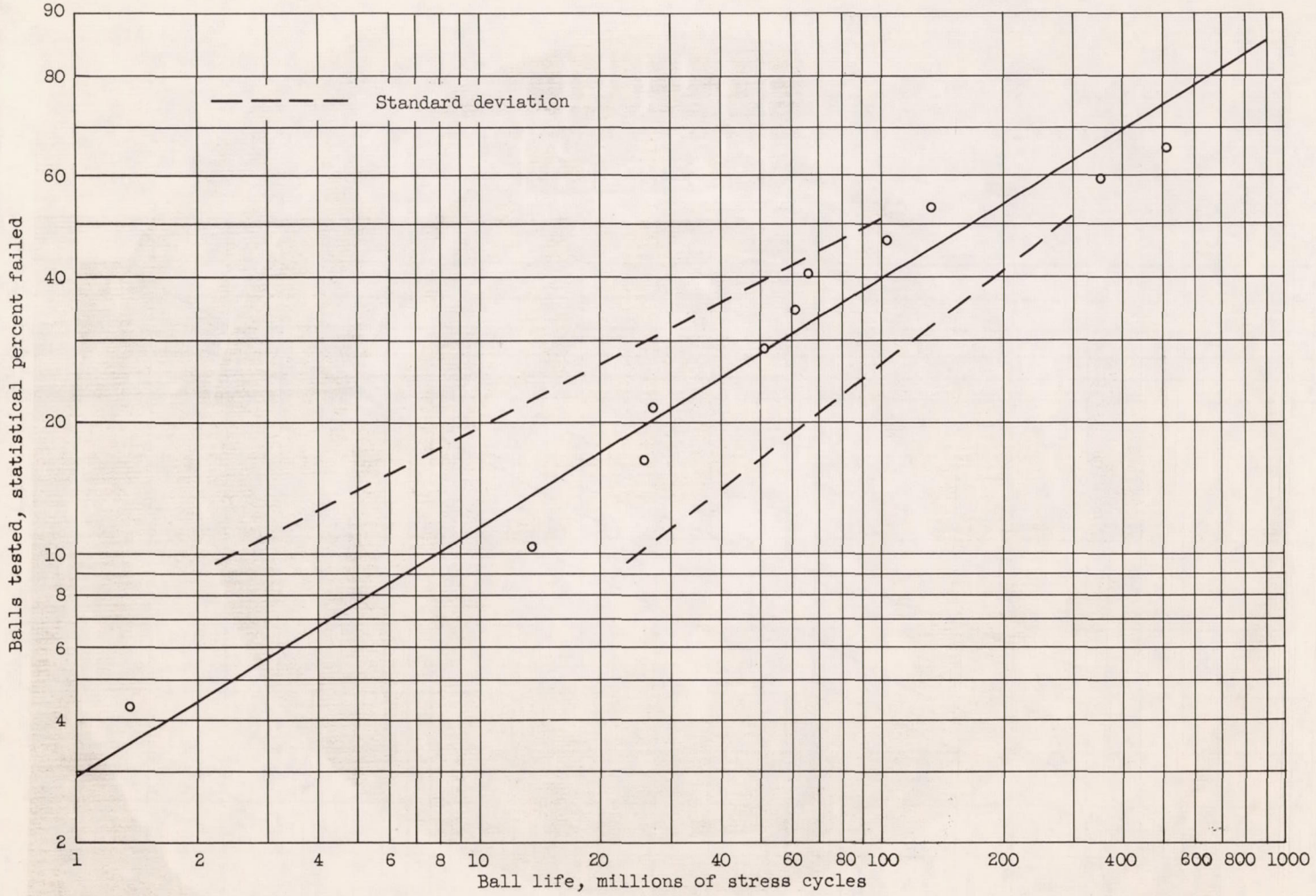

(a) Lubricant, polyalkylene glycol.

Figure 7. - Fatigue life for 1/2-inch AISI M-1 balls. Test temperature, 100° F; maximum Hertz compressive stress, 725,000 pounds per square inch.

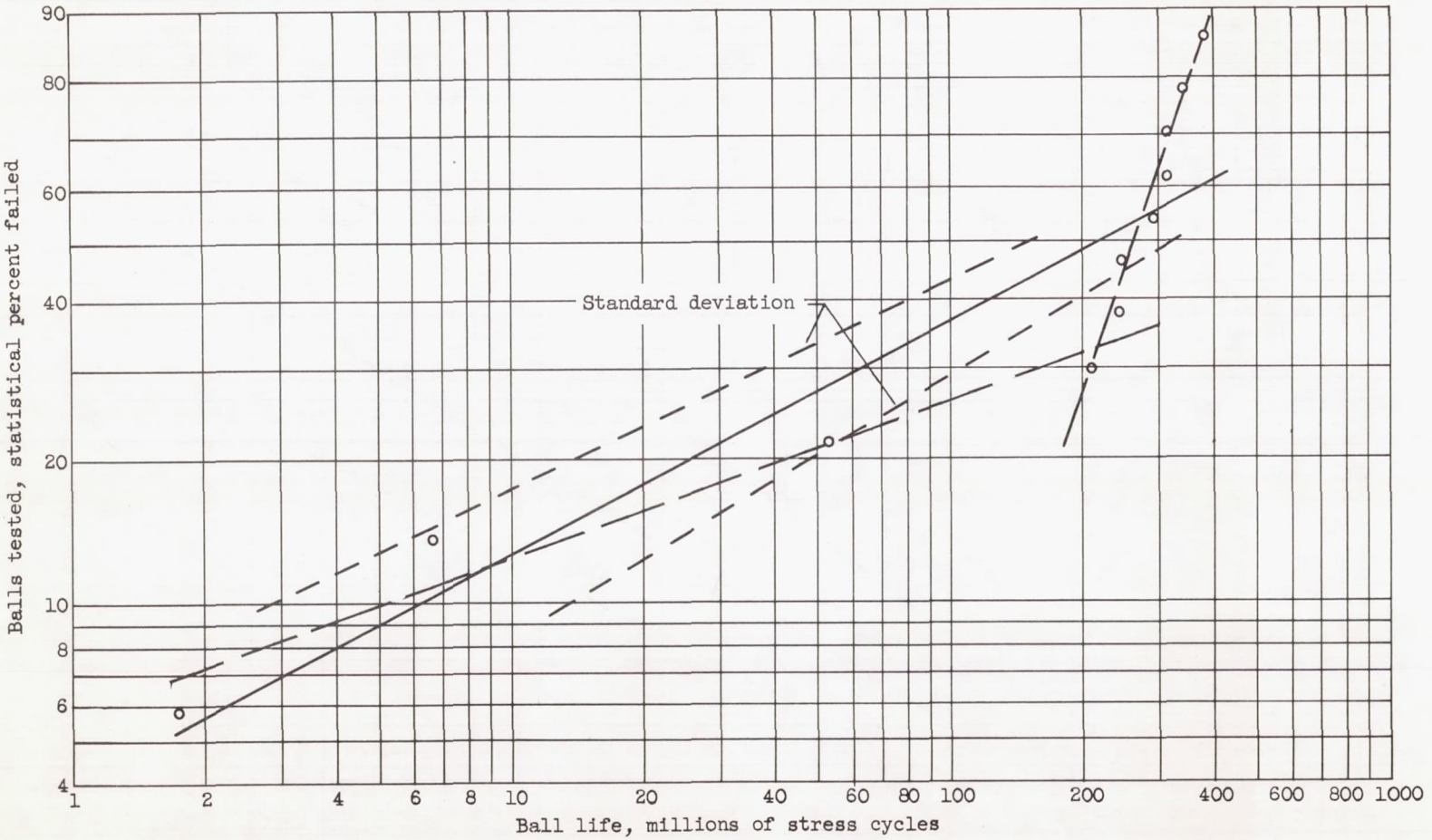

(b) Lubricant, 0.2-percent molybdenum disulfide suspension in polyalkylene glycol.

Figure 7. - Concluded. Fatigue life for 1/2-inch AISI M-1 balls. Test temperature, 100° F; maximum Hertz compressive stress, 725,000 pounds per square inch.

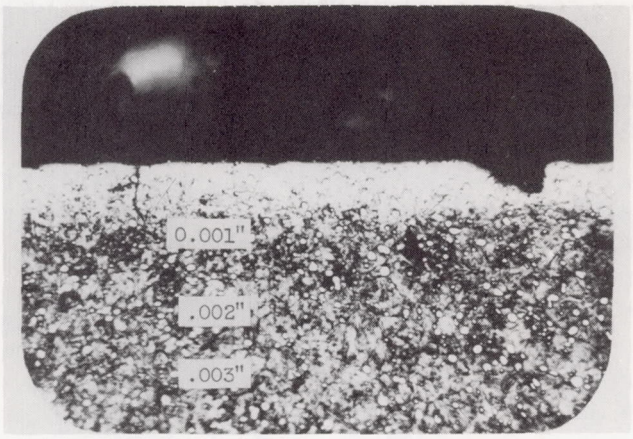

(a) Longitudinal section; X500; 53×10^6 stress cycles.

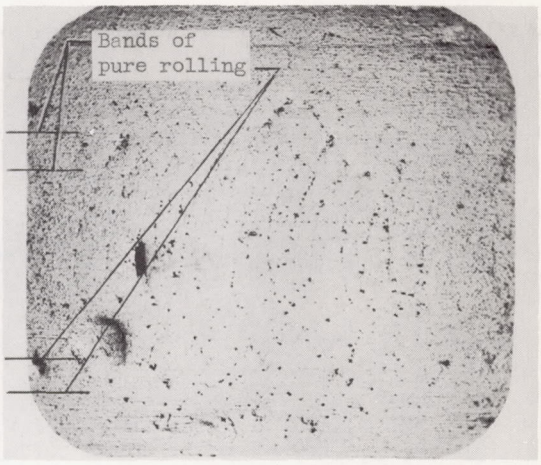

(b) Ball surface; X75; 53×10^6 stress cycles.

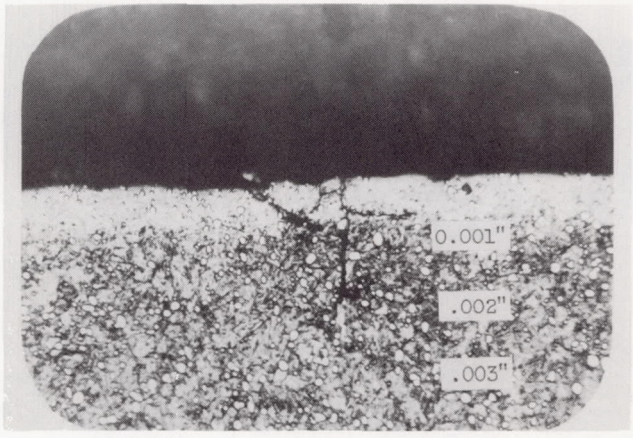

(c) Longitudinal section; X500; 210×10^6 stress cycles.

(d) Ball surface; X75; 210×10^6 stress cycles.

Figure 8. - Typical specimens. Lubricant, 0.2-percent molybdenum disulfide suspension in polyalkylene glycol; M-1 tool steel; test temperature, 100° F; maximum Hertz compressive stress, 725,000 pounds per square inch.

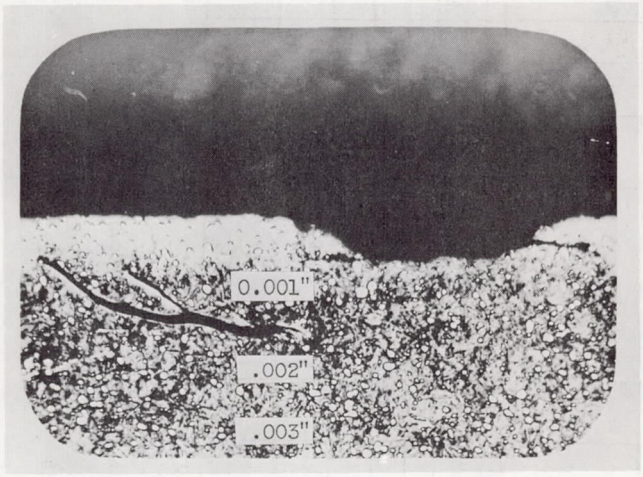

(e) Longitudinal section; X500; 330×10^6 stress cycles.

(f) Track surface; 330×10^6 stress cycles.

(g) Longitudinal section; X500; 53×10^6 stress cycles (unetched).

Figure 8. - Concluded. Typical specimens. Lubricant, 0.2-percent molybdenum disulfide suspension in polyalkylene glycol; M-1 tool steel; test temperature, 100° F; maximum Hertz compressive stress, 725,000 pounds per square inch.

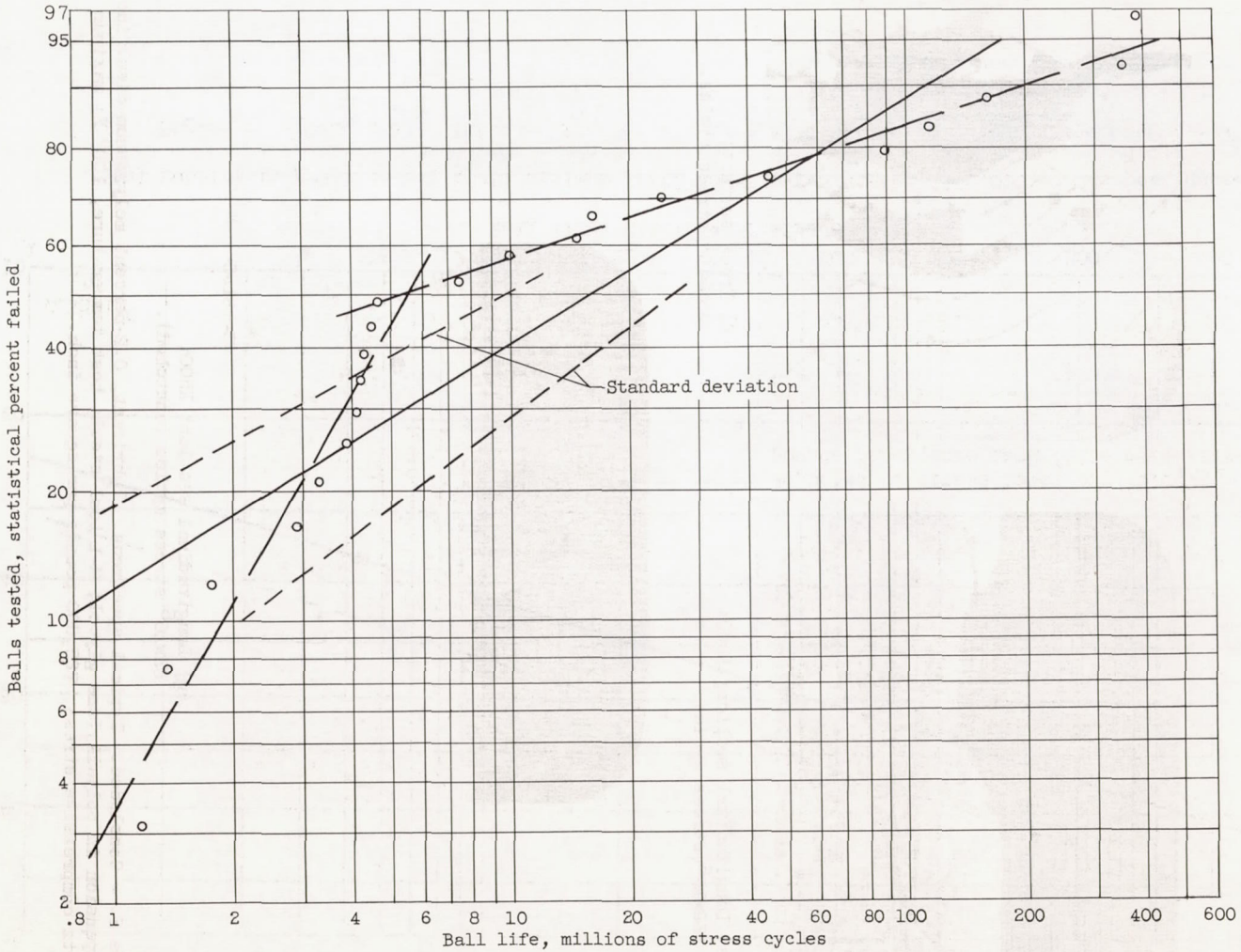

(a) Lubricant, 0.2-percent molybdenum disulfide suspension in polyalkylene glycol; maximum Hertz compressive stress, 725,000 pounds per square inch.

Figure 9. - Fatigue life for 1/2-inch AISI M-1 balls. Test temperature, 450° F.

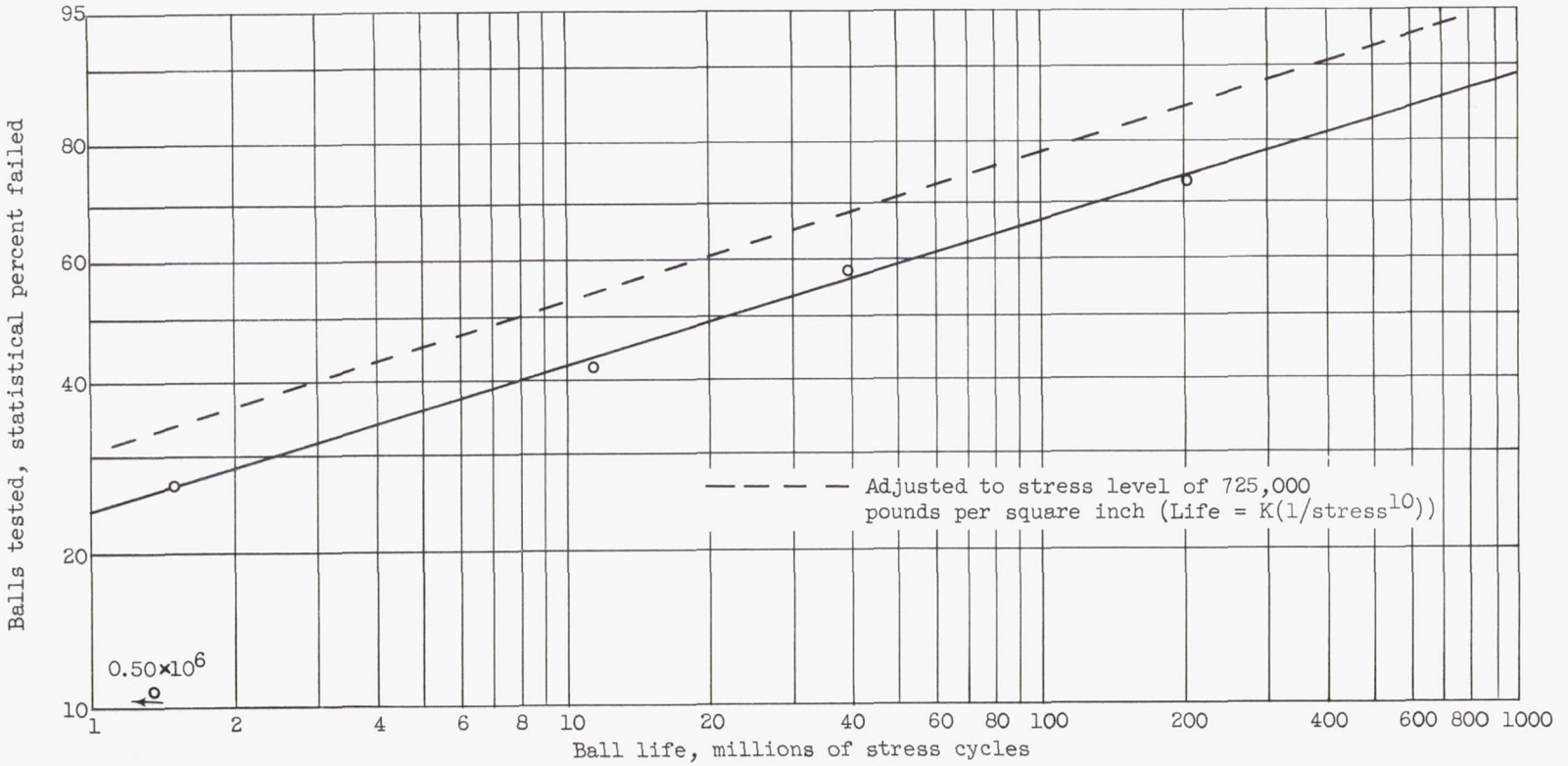

(b) Lubricant, graphite-air dust; maximum Hertz compressive stress, 650,000 pounds per square inch.

Figure 9. - Concluded. Fatigue life for 1/2-inch AISI M-1 balls. Test temperature, 450° F.

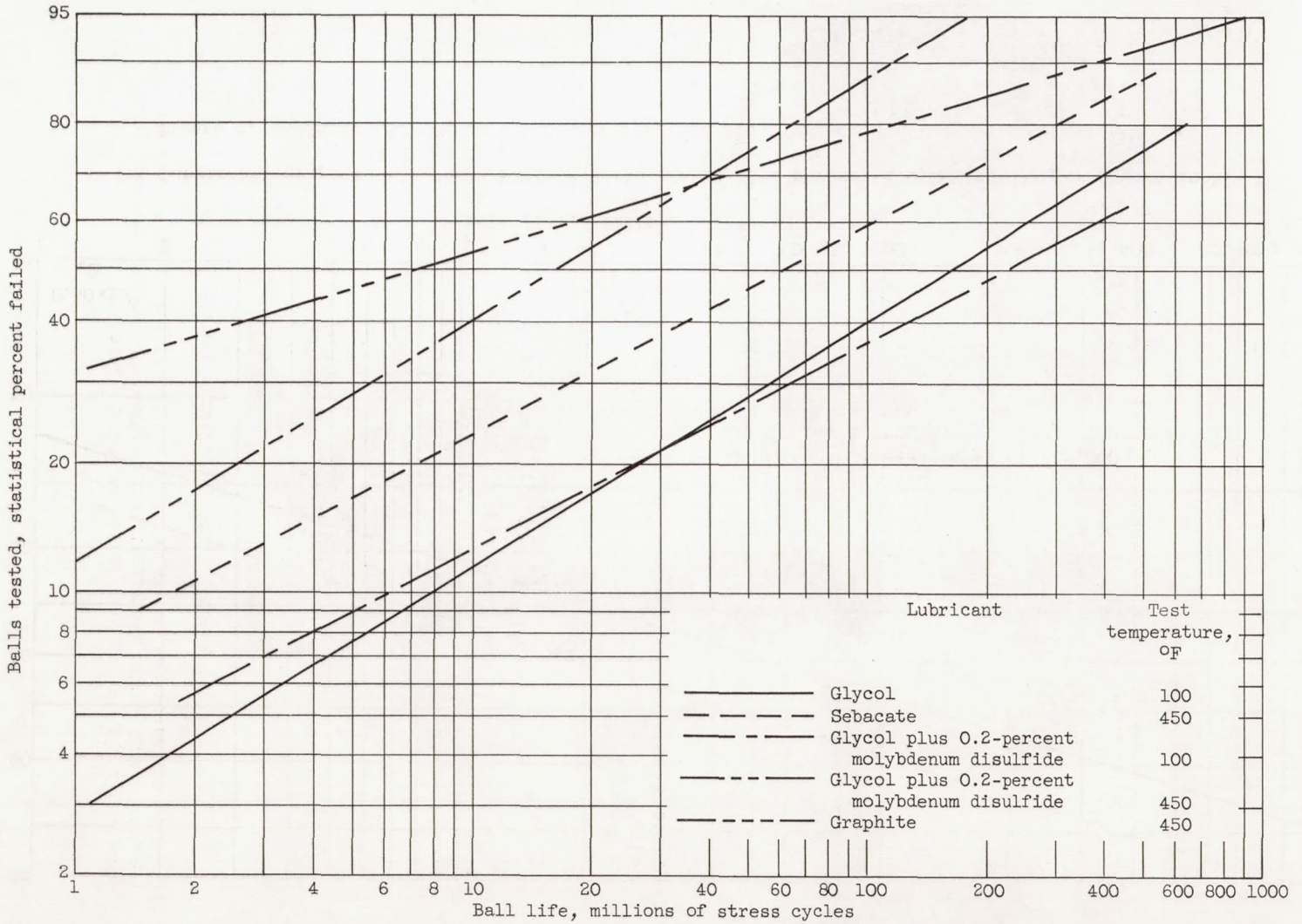

Figure 10. - Fatigue life for 1/2-inch AISI M-1 balls with various lubricants. Maximum Hertz compressive stress, 725,000 pounds per square inch.

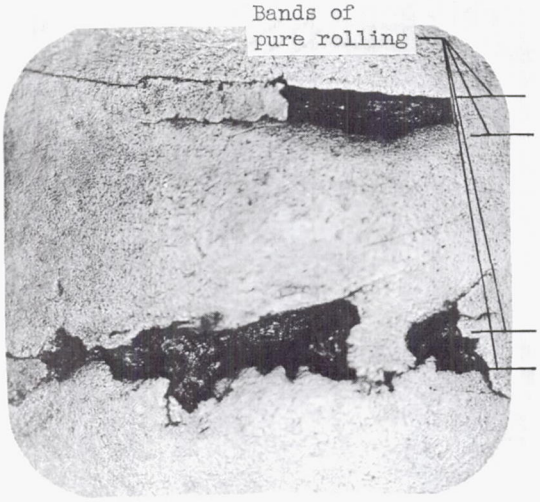

(a) Track surface; X75; spalling along bands of pure rolling.

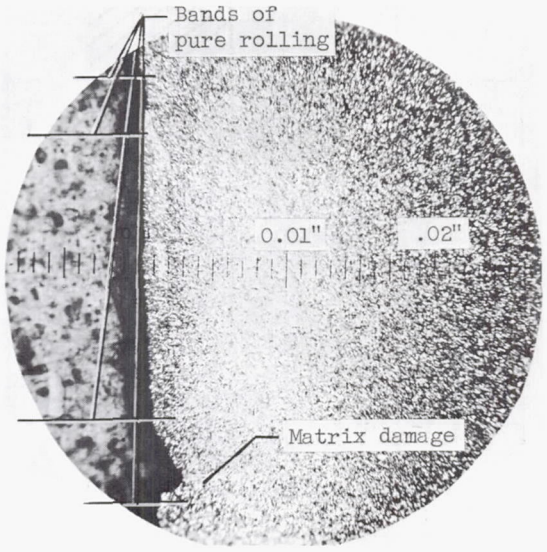

(b) Transverse section; X100; showing spalling and metallographic transformation.

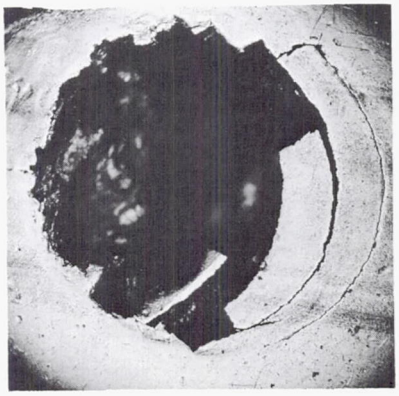

C-46194

(c) Typical fluid lubricant spall; X35.

Figure 11. - Typical dry powder failures. AISI M-1 tool steel; dry powder lubricant, molybdenum disulfide; test temperature, 450° F; maximum Hertz compressive stress, 725,000 pounds per square inch.

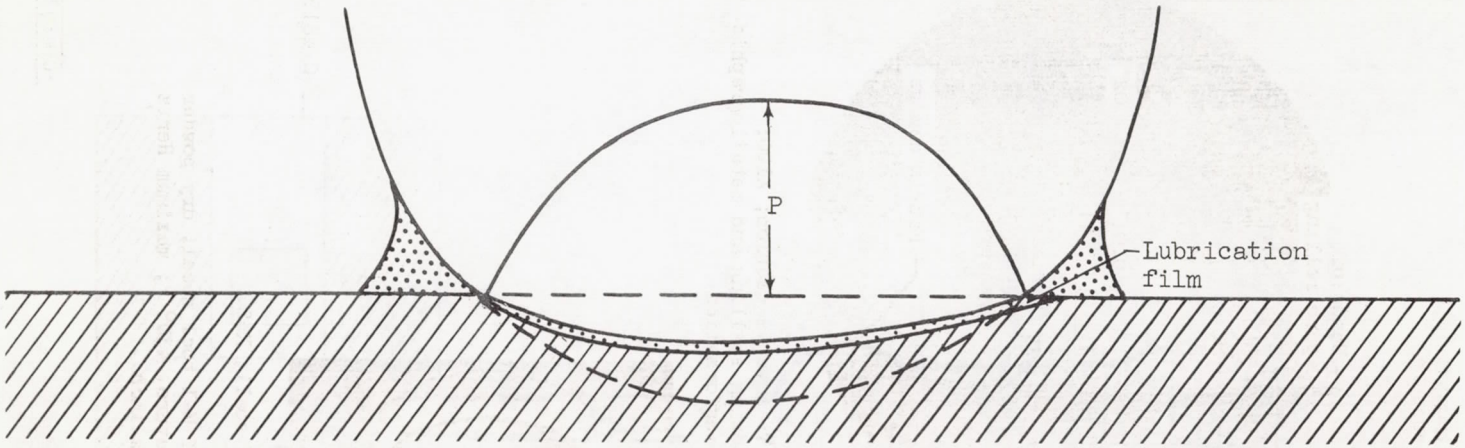

(a) Fluid lubricant.

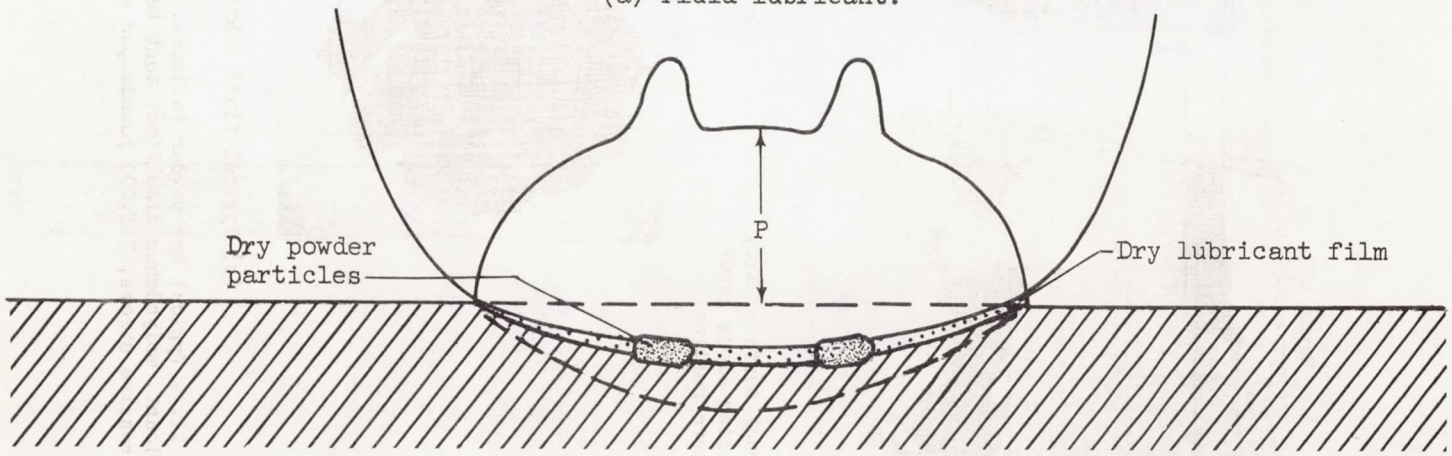

(b) Dry powder lubricant.

Figure 12. - Transverse section schematic diagram of pressure distribution in rolling sphere. Ball motion out of paper toward reader.

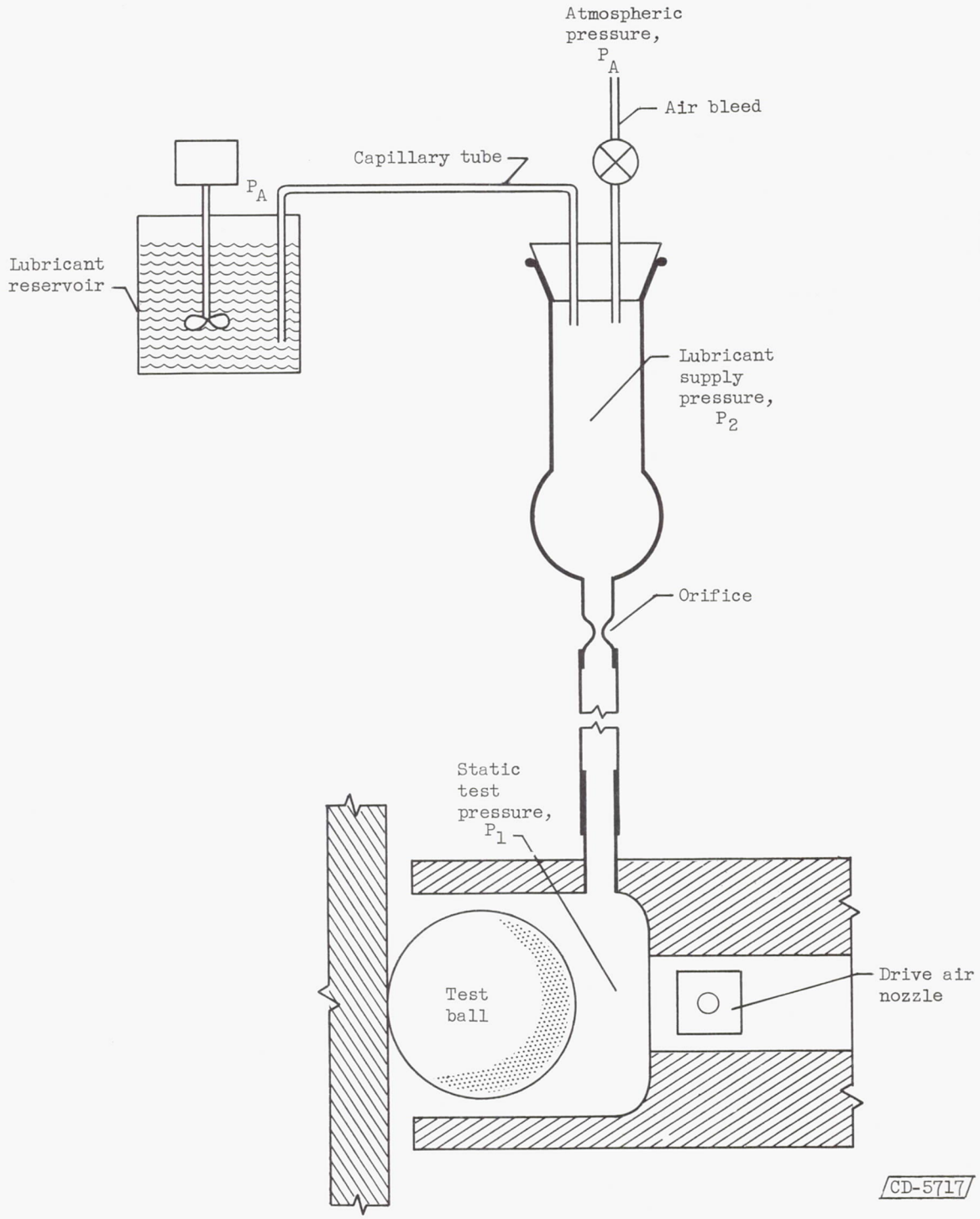

Figure 13. - Metering system for suspension lubricants.